POLITECNICO DI TORINO

Collegio di Ingegneria Chimica e dei Materiali

Master of Science Course
in Materials Engineering

Master of Science Thesis

Green *in situ* synthesis of silver nanoparticles on cellulose fibres by using sumac leaf extract

Tutor:
Prof. Ada Ferri
Co-tutor:
Prof. Brigita Tomšič

Candidate:
Elisa Savio

March 2020

Abstract

This study presents a simple and environmentally friendly method of producing an antimicrobial and UV protective finish on cotton fabrics using silver nanoparticles (Ag NPs) synthesised *in situ* by the green biochemical route. The synthesis of Ag NPs was carried out using *Rhus Thyphna* - sumac leaf extract both as a reducing and capping agent for silver nitrate ($AgNO_3$), which was used in five concentrations of 0.1 to 5.0 mM. The cotton fabric was pre-treated with an organic-inorganic hybrid sol-gel precursor to form a silica matrix on the fibres to improve the surface adsorption of Ag NPs and consequently a higher synthesis yield. The influence of the concentration of $AgNO_3$ used in the synthesis process on the morphological and chemical properties of the modified cotton fibres was investigated by scanning electron microscopy (SEM), energy dispersive X-ray spectroscopy (EDX) and inductively coupled plasma mass spectroscopy (ICP-MS). The functional properties of the investigated samples were assessed by colour measurements, the antibacterial activity against Gram-negative *Escherichia coli* and Gram-positive *Staphylococcus aureus* as well as the determination of UV-protection properties. The wash fastness of the newly synthesised Ag NPs was evaluated after one and five repeated washings. The results confirmed the successful formation of Ag NPs on the cotton fibres in the presence of sumac leaf extract with an average size of 70-100 nm. The Ag NPs were homogeneously distributed on the surface of the fibres and gave the cotton samples a light yellow to dark brown colour. The presence of Ag NPs caused an excellent 97% antimicrobial activity, which was higher for *S. aureus* than *E. coli*. This behaviour was attributed to the phenolic compounds in sumac leaf extract, which are strong antibacterial agents against Gram-positive bacteria, but proved to be a perfect breeding ground for Gram-negative bacteria. Accordingly, MIC against *E. coli* was 4.7 times higher than for *S. aureus*, but MBC was 340 mg/kg Ag, regardless of the bacterial species. As UV absorbers, Ag NPs in combination with sumac leaf extract provided excellent UV protection. While the presence of sumac leaf extract reflected only a UPF of 51, Ag functionalized cotton samples showed UPFs in the range of 40 to 69 as the concentration of $AgNO_3$ increased. The wash fastness of the newly synthesised Ag NPs was concentration dependent. In fact, five consecutive washes resulted in the loss of sufficient protection against *E. coli*, but the excellent antibacterial activity against *S. aureus* of R<90% was still retained in the sample treated with 5.0 mM $AgNO_3$. After five laboratory washes, the UPF values of the samples also decreased. However good to excellent UV protection was still maintained with an UPFs of 30 to 40. Accordingly, the proposed *in situ* synthesis of Ag NPs using sumac leaf extract proved to be not only environmentally friendly, but also promising to produce textiles with multifunctional antibacterial and UV-protective properties in a very simple way with satisfactory wash fastness of the synthesized Ag NPs.

Sommario

Inquadramento teorico e obbiettivi

La crescente consapevolezza della minaccia di agenti patogeni sulla salute umana sta portando a una sempre maggiore richiesta di prodotti antimicrobici in diversi campi tra cui tessuti, dispositivi medici, impianti di filtrazione per aria e acqua, imballaggi alimentari. I tessuti sono tra campi che più beneficiano di questo tipo di funzionalità. Largo impiego di rivestimenti antimicrobici può essere fatto in ambiente ospedaliero piuttosto che in edifici pubblici per evitare la diffusione di virus e batteri pericolosi per la salute. L'azione biocida su tessuti intimi o sportivi riduce la possibilità dello sviluppo di cattivi odori e diminuisce il numero di lavaggi sulla vita del singolo capo, riducendone l'impatto ambientale. Inoltre, la proliferazione di batteri e muffe potrebbe compromettere l'integrità stessa delle fibre, portando a un significativo cambio delle caratteristiche estetiche e delle proprietà fisiche del tessuto. Questi tipi di agenti devono però soddisfare numerose restrizioni per porsi competitivamente sul mercato: non devono alterare la microflora della pelle, devono essere economici e facilmente applicabili, resistenti a lavaggio, e non devono apportare modifiche estetiche o fisiche al tessuto. Nonostante le numerose limitazioni, diversi agenti sono già stati individuati, tra i quali, le nanoparticelle di argento (Ag NP) risultano tra i più efficaci. Queste ultime sono state testate essere un potente biocida contro una vasta gamma di batteri, virus, funghi. L'azione battericida delle nanoparticelle di argento è stata lungamente dibattuta dalla comunità scientifica e ancora non è chiaro quali siano i principali meccanismi di sviluppo. Si ipotizza che questa sia il risultato di un'azione congiunta di più fattori: il contatto tra la parete cellulare e le nanoparticelle, il rilascio dalla superficie di queste ultime di cationi metallici per ossidazione in ambiente acquoso, e la creazione di ROS. Tutti questi meccanismi portano a una progressiva compromissione delle funzioni basilari per la vita della cellula e alla perdita della permeabilità della membrana cellulare, con conseguente rottura e fuoriuscita del materiale citoplasmico. Molti sono i fattori che incidono sui risultati di tale processo. Primo fra tutti la taglia delle nanoparticelle. Numerosi studi infatti hanno evidenziato un aumento dell'attività antibatterica legato a una diminuzione di taglia e, indagini al microscopio elettronico a trasmissione, hanno rivelato la possibilità per le particelle di dimensione inferiore a 10 nm di penetrare la membrana cellulare. Anche la forma delle NP è stata indagata in relazione al fenomeno: le facce cristalline a più alta densità atomica {111} risultano quelle più reattive al rilascio di cationi e alla formazione di specie reattive. Inoltre, un altro importante fattore da tenere in considerazione è l'agente stabilizzante utilizzato per la dispersione delle particelle in fase di sintesi. Gli agenti surfattanti influiscono sul processo di aggregazione e conferiscono alla particella una carica superficiale che può portare a un miglioramento o peggioramento della sua attività antibatterica.
Il processo di produzione delle Ag NP può avvenire attraverso processi top-down o bottom-up, per via chimica o fisica. Tra i processi più utilizzati si fanno strada la precipitazione chimica, anche attraverso l'uso di micro-emulsioni o per via fotochimica, oppure metodi come l'ablazione laser o il processo di evaporazione e condensazione. Tali metodi si contraddistinguono per un consumo di energia elevato, macchinari costosi o agenti chimici tossici per l'ambiente. Negli ultimi anni un nuovo processo di sintesi sta catturando l'attenzione dei ricercatori per la sua semplicità e economicità. Come nel processo di

precipitazione chimica tradizionale sono coinvolti tre componenti: un sale di argento, un agente riducente e un agente stabilizzante. Nel caso della sintesi biologica di Ag NP, l'agente riducente e l'agente stabilizzante possono essere ricavati da batteri, funghi, lieviti, alghe o piante. Lo scopo di questo studio è quello di indagare in tale ambito una nuova tecnica di sintesi *in situ* per la produzione di Ag NP su fibre di cotone, utilizzando come agente riducente e stabilizzante estratto di foglie di sumac. La specie Rhus, più comunemente conosciuta come sumac, è parte della famiglia delle Anacardiaceae, che conta più di 250 specie al suo interno, e cresce in varie zone del mondo, dal nord America, sud Africa, Asia, bacino mediterraneo. I campioni in cotone sono stai impregnati con una matrice polisilossanica per incrementare la durabilità del rivestimento. Sono state utilizzate varie concentrazioni di $AgNO_3$, utilizzato come precursore delle particelle durante il processo di sintesi, per valutare le funzionalità del prodotto in diepndenza dalla concentrazione iniziale di argento. La resistenza a lavaggio del rivestimento è stata valutata dopo uno e cinque lavaggi in laboratorio, utilizzando analisi colorimetriche. La struttura superficiale è stata caratterizzata con microscopio a scansione elettronica (SEM), spettroscopia EDS (energy-dispersive X-ray spectroscopy), plasma accoppiato induttivamente (ICP-MS). L'attività antibatterica è stata testata contro i batteri Gram-positivo (*Staphylococcus aureus*) e Gram-negativo (*Escherichia coli*). Inoltre, sono state valutate le capacità dei campioni di schermare la radiazione UV tramite la misurazione del fattore di protezione UPF.

Parte sperimentale

La produzione in situ delle Ag NP è stata realizzata attraverso tre step. Il primo passo ha portato alla creazione di una matrice polisilossanica sulle fibre di cotone, con lo scopo di migliorare l'adesione delle NP. Un precursore organico-inorganico sol-gel è stato idrolizzato in acqua (15 g/L) e applicato al tessuto utilizzando una tecnica pad-dry-cure.
Il secondo passo ha previsto la produzione dell'estratto di foglie di sumac. Le foglie essiccate all'aria sono state finemente sminuzzate a mano e, in proporzione 20 g/L, messe a bollire in acqua per 20 min. Infine, i campioni pretrattati di cotone sono stati immersi, in rapporto solido:liquido 1:25, in soluzioni di $AgNO_3$, preparate in cinque differenti concentrazioni: 0.1 mM, 0.5 mM, 1.0 mM, 2.5 mM, 5.0 mM. Il pretrattamento è stato realizzato in un apparecchio Gyrowash per 10 min a 60°C. L'estratto di sumac è stato aggiunto a ogni campione raggiungendo un rapporto solido:liquido 1:50 e il la sintesi è avvenuta nell'apparecchio Gyrowash per 1 h a 60°C.
Per determinare la resistenza al lavaggio, i campioni sono stati sottoposti a un trattamento nel macchinario Gyrowash, in modo tale da rendere ogni lavaggio equiparabile a 5 lavaggi domestici (norma ISO 105-C06) utilizzando 10 palline di acciaio in ogni capsula di lavaggio. Ogni ciclo di lavaggio è stato performato a 45°C per 45 min. Alcuni dei campioni hanno subito un solo ciclo di lavaggio, altri sono stati trattati cinque volte ripetutamente.
Per caratterizzare morfologicamente i campioni ottenuti, le seguenti tecniche sono state utilizzate: microscopio a scansione elettronica (SEM), spettroscopia EDS (energy-dispersive X-ray spectroscopy), plasma accoppiato induttivamente (ICP-MS). Sono seguite analisi colorimetriche, analisi antibatteriche (AATCC 100) contro i batteri Gram-negative *Escherichia coli* e Gram-positive *Staphylococcus aureus* e la misurazione della protezione alla radiazione UV del tessuto.

Analisi e risultati

La morfologia e la qualità della dispersione delle NP di argento è stata valutata attraverso il microscopio a scansione elettronica con elettroni retro riflessi (SEM-BSE). Dalle micrografie (Figura 3.1) è stato possibile vedere la crescita del contenuto di NP su campioni trattati con crescenti concentrazioni di $AgNO_3$ nel processo di sintesi. Di conseguenza, sulla superficie del campione trattato con la minore concentrazione, 0.1 mM, sono state rilevate poche NP, piccole e ben disperse, e tra le fibre non sono stati trovati aggregati. Al contrario, il campione trattato con 5.0 mM $AgNO_3$ ha mostrato la più alta

concentrazione di nanoparticelle sulle fibre e all'interno della trama. Dalle immagini EDS (Figura 3.3), che hanno confermato l'effettiva presenza delle NP di argento sulla superficie del tessuto, è risultata una buona omogeneità di distribuzione sulle fibre. Attraverso il software Image J, utilizzando le immagini SEM-BSE (10 kV), sono state analizzate le dimensioni e la distribuzione di taglia delle particelle (Figura 3.2). La variazione di concentrazione di $AgNO_3$ utilizzato in fase di sintesi esercita un diretto effetto sul diametro delle NP, a partire da 70 nm per il campione sintetizzato con 0.5 mM di $AgNO_3$, fino a più di 100 nm per la più alta concentrazione di $AgNO_3$, 5.0 mM. Più alta è la quantità di particelle, maggiori sono le dimensioni misurate, in virtù del processo di agglomerazione durante la loro deposizione sulle fibre. Inoltre, anche la distribuzione di taglia risulta più larga all'aumentare dalla concentrazione di $AgNO_3$. L'analisi ICP-MS è stata realizzata sui campioni contenenti argento, sia prima che dopo i ripetuti cicli di lavaggio, per verificare l'effettiva concentrazione del metallo depositato sulle fibre. Come atteso dalle precedenti analisi un aumento nella concentrazione di $AgNO_3$ nel processo di sintesi porta a una maggiore concentrazione di argento sul cotone. I numerosi cicli di lavaggio causano la perdita di NP dalle fibre, soprattutto dove il contenuto di metallo risulta più alto, probabilmente a causa del facile rilascio degli aggregati più voluminosi.

Le analisi colorimetriche hanno riportato un notevole cambiamento di colore, valutato attraverso le coordinate CIE L^*, a^* e b^*. La resistenza del colore al lavaggio è invece stata determinata tramite la misurazione della differenza di colore tra i campioni prima e dopo lavaggio (ΔE^*). Le indagini colorimetriche hanno riportato una colorazione giallastra dovuta alla presenza dell'estratto di foglie di sumac, portata verso tonalità più scure rosso brunastro in presenza dell'avvenuta sintesi di nanoparticelle (Figura 3.6 e Tabella 3.1). Tonalità rosso-bluastro si sono presentate con l'aumento della concentrazione di queste ultime. Questo cambio di colore sui campioni studiati ha portato a un conseguente diminuzione della luminosità. A seguito dei lavaggi i campioni hanno riportato una diminuzione della luminosità e tonalità bluastre. Tuttavia, è stato possibile rilevare un facile desorbimento dalle fibre sia dell'estratto naturale, sia delle nanoparticelle, con maggiori differenze nei campioni a più alta concentrazione di Ag, probabilmente dovuto al facile distacco degli aggregati più voluminosi. Per molti dei campioni ΔE^* (Figura 3.7) è risultato maggiore di 5.0, confermando una pessima resistenza del colore.

L'attività antibatterica dei campioni trattati con le Ag NP, prima e dopo il lavaggio, è stata valutata contro il batterio Gram-negativo *E. coli* (Figura 3.9) e il batterio Gram-positivo *S. aureus* (Figura 3.10). I campioni di cotone non hanno mostrato nessuna attività antimicrobica mostrandosi un substrato ideale per la crescita dei batteri. L'estratto di sumac ha rivelato eccellenti proprietà antibatteriche contro *S. aureus* (R>97%), ma non ha portato alla riduzione della crescita di *E. coli*, risultando in valori negativi di R (R<-20%). L'attività antibatterica delle Ag NP sembra lavorare sinergicamente con l'estratto di sumac, portando a un'eccellente riduzione della crescita di *S. aureus* (R>98%) per tutti i campioni, indipendentemente dalla quantità di nitrato d'argento utilizzato nel processo di sintesi. Al contrario, per ottenere una sufficiente protezione contro il batterio *E. coli*, maggiori concentrazioni di $AgNO_3$ e quindi di Ag NP sono richieste. A conferma di ciò, comparando i risultati di riduzione delle colonie con i risultati ottenuti dalle analisi ICP-MS (Figura 3.11) emerge che la concentrazione inibitoria minima (MIC) per il batterio Gram-positivo (15 mg/kg) risulta 4.7 volte inferiore rispetto a quella del batterio Gram-negativo (70 mg/kg). La concentrazione minima biocida (MBC) invece, appare essere per entrambi i batteri la medesima (340 mg/kg). I ripetuti lavaggi mostrano chiaramente una resistenza della funzionalità del tessuto dipendente dalla concentrazione iniziale: maggiore è la concentrazione iniziale, maggiore è l'attività antimicrobica dimostrata dopo lavaggio. Cinque lavaggi consecutivi hanno tuttavia comportato la perdita della resistenza al batterio *E. coli* (R<60%), mentre l'attività antibatterica contro *S. aureus* si è preservata eccellente (R>90%) per i campioni trattati con la più alta concentrazione di $AgNO_3$ nel bagno di sintesi.

La radiazione ultravioletta si può localizzare tra i 200 nm e i 400 nm a si può classificare in tre regioni UVA (tra 320 e 400 nm), UVB (tra 280 e 320 nm) e UVC (200 e 280 nm), L'area UVC, che sarebbe la più pericolosa per l'uomo, è completamente assorbita dallo strato di ozono che circonda la terra, perciò l'azione protettiva alla radiazione UV del tessuto e delle fibre è principalmente attribuita alla resistenza nella regione UVA e UVB. Il cotone non ha presentato proprietà di protezione ai raggi UV, con un valore di UPF di 3.8 (Tabella 3.2). L'estratto di foglie di sumac, grazie ai composti fenolici presenti al suo interno, si è rivelato un'ottima barriera alla penetrazione della radiazione UV, con un valore di UPF di 51.11. La presenza delle NP ha portato a una decrescita delle performance. Un'azione sinergica tra l'estratto e le NP è invece stata osservata per i campioni trattati con concentrazioni di $AgNO_3$ superiori a 1.0 mM che hanno portato a misurazioni di UPF superiori a 55.7. In questo caso le Ag NP hanno agito assorbendo la radiazione UV, migliorando la protezione già offerta dall'estratto naturale di foglie di sumac diminuendo trasmissione e riflessione nella regione spettrale UVA (320-400 nm). Le proprietà di protezione diminuiscono dopo ripetuti lavaggi così come già confermato dai risultati delle analisi colorimetriche e antibatteriche (Figura 3.12). Il lavaggio dei campioni ha portato a una leggera decrescita del fattore protettivo, mostrando tuttavia soddisfacenti performance, con UPF>30.

Conclusioni

Lo studio effettuato conferma che l'estratto di foglie di sumac si presenta come un'interessante alternativa ai tradizionali prodotti riducenti e stabilizzanti per la produzione di rivestimenti di Ag NP su cotone. Il processo si contraddistingue per la sua semplicità, basso costo e compatibilità ambientale. L'estratto naturale ha mostrato una colorazione giallastra sul tessuto, eccellenti attività antimicrobiche e alti valori di UPF, tuttavia il suo desorbimento durante il processo di lavaggio non preserva le sue funzionalità nel tempo. Inoltre, ottime proprietà antibatteriche e di protezione ai raggi UV sono state ottenute dai prodotti trattati con Ag NP. Ulteriori ricerche sono però necessarie per migliorare la stabilità delle NP sulle fibre durante i lavaggi. L'adesione attraverso legami fisici delle NP alla matrice ha portato a miglioramenti assicurando eccellente schermatura ai raggi UV anche dopo cinque lavaggi, ma non è risultato sufficiente per impartire una protezione contro i batteri Gram-negativi, anche se ottimi risultati sono ancora visibili contro i Gram-positivi.

Acknowledgements

This research was carried out at the Department of Textiles, Grapghic Arts and Design of the Faculty of Natural Sciences and Engineering, University of Ljubljana. The research was cofounded by the EU project UIA02-228 APPLAUSE (Alien Plant Species from harmful to useful with citizens' led activities) and the Slovenian Research Agency (Program P2-0213, Infrastructural Centre RIC UL-NTF).

I would like to thank my supervisor Ada Ferri for this thesis opportunity that gave me the occasion to live an interesting experience abroad. I need to express my deepest gratitude to my co-supervisor Brigita Tomšič, for hosting me in the University of Ljubljana, in a talented research group, whose members were very kind and helpful with me, and for helping to write this master thesis. I would also thank Danaja Štular who helped me to carry out my experimental work, with great patience and support.

Therefore, I need to write a sincere and lovely thanks to all my family for the comprehension and the encouragement they gave me in moments of difficulty, and for giving me the opportunity to chase my dreams with all the support that I need every day.

Finally, a special thanks is for my friends, the one I grew up with in my hometown, but also for those who I met living on my own, who became my second family. Despite the distance, their support has been fundamental.

Contents

List of Figures

List of Tables

Introduction

Public awareness about effects of pathogens on health creates a growing demand about antibacterial active materials in various fields such as textiles, medical devices, hygienic applications, water purification systems, and food packing [Iyigundogdu et al., 2017]. Fibres, especially when in contact with skin, supply an outstanding breeding grounds for microorganisms in presence of favourable conditions of moisture, heat, dirt and possibility of nutrients supply, often coming from the fibres themselves. Not surprisingly, natural fibres are more subject to the microorganism attack since they work by secreting specific enzymes that can break down cellulose (in cotton, flax and others), and degrade proteins (in wool and other animal hair fibres) to turn them into nutrients. On the other hand, synthetic fibres, by virtue of their very un-natural origins, that leads to a different spacing in carbon atoms, are not greatly affected by microorganisms [Dhende et al., 2012]. Offering a product capable of inhibiting proliferation (biostatic) or killing microorganisms (biocidal) i.e., bacteria, viruses, fungi and protozoa during use and storage, is intended to protect the possible wearer as well as the textile itself. Indeed, pathogenic and odour-causing microorganisms can lead to health and hygiene problems for humans, a concern both in medical applications and in everyday life. Hospitals, nursing homes, schools, hotels, and crowded public areas can benefit from antimicrobial finishing to prevent the danger of infection from pathogens, while intimate apparel, underwear, socks and athletic wear are an important market to control individual's malodours produced by the bacterial decomposition of sweat and other body fluids [Schindler and Hauser, 2004]. Furthermore, textile substrates can be subjected to aesthetic changes such as coloured stains and discoloration and biodegradation due to moulding and rotting, which results in the reduction of breakage strength, elongation and elasticity and can lead to reduced use value of textiles [Gao and Cranston, 2008, Schindler and Hauser, 2004, Dring, 2003, Simoncic and Tomsic, 2017]. In this regard, antimicrobial finishes are particularly important for fabrics that are exposed to weather as the ones used for awnings, screens, tents, tarpaulins, ropes, as well as home furnishings (carpets, curtains, mattress ticking and upholstery), fabrics that have to be stored or shipped under critical condition of heat and humidity or textile left wet between processing steps for an extended time.

Antimicrobial agents should be effective against a broad spectrum of undesirable microorganisms, which is becoming more and more important and new toxicity standards and production limitation increase the requirements that have to be fulfilled to create a competitive product on the market. Accordingly, antimicrobial agents should exhibit low toxicity to consumers, not cause allergy or irritation and preserve the skin microflora, which is important for the pH balance and the antibiotics production of the skin that is the first line of defence against pathogenic bacteria [Elsner, 2006, Gao and Cranston, 2008]. Antimicrobial agents should be effective at low concentrations and have low contact time in the whole life cycle of the textile product. Furthermore, is important for the product not to affect the appearance of the fabric, being colourlessness and odourlessness, and not to change any of its intrinsic mechanical and physical properties. The antimicrobial finishing should be durable to various cleaning and ironing processes since as a textile product is subjected

to repeated washing during its life time. Finally, antimicrobial agent should show compatibility with other finishing agents and auxiliaries, ease of application through standard set up of textile machinery [Dhende et al., 2012], economical use and not produce harmful substances to the manufacturer and the environment [Dring, 2003, Simoncic and Tomsic, 2017, Borsa, 2012]. Despite the long list of requirements, up to now various kind of antimicrobial agents with diverse structures such as organometallics, heavy metal ions, phenols, formaldehydes, quaternary ammonium salts, chitosan, synthetic dyes, organosilicones and natural dyes have been used to impart demonstrable antimicrobial properties to textile materials [ul Islam et al., 2016]. Antimicrobial agents can be divided in two categories according to their mechanism of antimicrobial activity: a controlled-release and a bio-barrier formation mechanism [Simoncic and Tomsic, 2017]. According to the first mechanism antmicrobial agent gradually leach from the textile into their surroundings in the presence of moisture, where they act as a poison for microorganisms [Simoncic and Tomsic, 2017]. This type of finishing agents can be physically incorporated into the textile fibres and among the most important, we can find halogenated phenols, cationic surfactants known as quaternary ammonium (QAS) and phosphonium (QPS) salts, zinc pyrithione, polybiguanides, N-halamines, nanoparticles of noble metals and metal oxides, and natural plant-based bioactive substances. On the other hand, a bio-barrier formation mechanism includes unique chemical structures that act as inert physical barrier coating material or surface coatings which can kill microbes on contact. The most important bio-barrier formation antimicrobial agents used for the chemical modification of textiles include polymerizable surfactants (surfmers), QAS-functional trialkoxysilanes, reactive dyes with incorporated QAS and reactive quaternized chitosan [Simoncic and Tomsic, 2017]. Chemical binding of these agents to the textile surface can also be possible, but only if there are enough reactive functional groups in the agent and in the fibres to form chemical bonds. The concentration of the active compound within the antimicrobial agent is crucial for its antimicrobial activity, regardless of the type of the mechanisms of action. It is well known that the minimum inhibitory concentration (MIC) is required for biostatic activity, while the minimum biocidal concentration (MBC) should be exceeded for biocidal activity [Schindler and Hauser, 2004]. As the concentration directly influences the efficiency of antimicrobial agent, it should not be below the MIC. In this respect, important disadvantage of antimicrobial agents that act according to controlled-release, is their continuous leaching from the fibres during the use of the functionalized textile product as well as during repetitive laundering. Accordingly, gradual but persisting leaching of the antimicrobial agent results in a decrease of the concentration of the active substance, which eventually falls below MIC and thus below the limit of effectiveness. This give the possibility for microorganisms to develop resistance against such antimicrobial agent. Furthermore, the release of the toxic substance could negatively affect skin microflora and leaching in washing cycles could rise environmental pollution concerns. Some of these finishing can be subjected to a regeneration principle that means the finish can be reactivated by some additional step after use. Antimicrobial agents that form bio-barrier have some significant advantages over the leaching ones. Because of their non-leaching properties, the concentration of the active substance does not decrease, which results in a very small probability for microorganisms to develop resistance to them. The bio-barrier formation enables only the microorganisms that are adsorbed onto the textile surface to be killed, so the agents cannot cross the skin barrier and irritate the skin. Bound antimicrobials are much more resistant to repeated laundering compared to leaching agents. Along with these advantages, however, these agents also demonstrate an important weakness. Namely, despite the presence of the barrier on the fibre surface, these can be deactivated by deadly microorganisms, the adsorption of dirt or the neutralization of positive charges owing to complex formation between the cationic antimicrobial group of the biobarrier and the anionic detergent during laundering. Additionally, the bio-barrier can be gradually removed from the fibre surface by abrasion.

Among different antimicrobial agents, silver nanoparticles (Ag NPs) have become the most widely

represented and studied inorganic antimicrobial agent in recent years, responding to a controlled-release mechanism. They've been proved being effective on a great variety of microorganism and it seems to offer the best option to antibiotic-resistant bacteria thanks to the synergic action of Ag NPs and Ag^+ cations released in the surroundings medium which damage cell walls or alter cell membrane permeability, denature proteins, inhibit enzyme activity, or inhibit lipid synthesis compromising the cell survival. The efficiency of Ag NPs is thus depending on several factors such as size, shape, surface charge, surface coating, which makes every parameter in the process of production essential for the final effectiveness of the product and the critical concentration for showing its toxicity [Xiu et al., 2012]. Nevertheless, antimicrobial effects of Ag NPs appear like a double-edged sword: cytotoxicity, genotoxicity, immunological response, and even cell death are some of the negative effects that are still under evaluation, with the aim to prevent unpredictable interactions of Ag NPs with the biological system [Akter et al., 2018]. In the chemical modification processes of textile materials, application of Ag NPs is performed according two different techniques. The first, *ex situ*, consist in producing the Ag NPs according to physical or chemical method, and applying them in a second step to the textile, using an appropriate finishing method, i.e. impregnation or exhaustion. The *in situ* method on the contrary, proceeds in one step, whereas nucleation and growth of the Ag NPs occur directly on the surface of the fibres. The second technique is preferable over the first one, because of minimized agglomeration of Ag NPs as well as increased homogeneity and uniformity of Ag NPs distribution, reflecting in the creation of more stable and durable coating [Shaheen and Aty, 2018]. Nevertheless, production of Ag NPs is often associate with the employment of toxic chemicals used as reducing and stabilizing agents or high energy requirements, which are rather difficult and including wasteful purifications [Ahmed et al., 2016]. Their toxicity for the environment and undesirable effects on the fabric making it inappropriate for medical usage, are the main reason for increasing effort of the researchers to develop process for green synthesis of Ag NPs. Such green synthesis includes the use of naturally derived reducing and stabilizing agents, like plants (i.e. bark, branches, roots, leaves, seeds and fruits) extract, in no toxic solvents, i.e. water or alcohol. Results achieved so far are encouraging for operational simplicity, high yield, matching less generation of toxic substances. Furthermore, the possibility to choose the natural source can enhance the efficiency of the products, since, plants with reported medicinal/antibacterial properties negotiate the synthetic cues while the unused metabolites adds further to their anti-microbial/medicinal properties [Jha and Prasad, 2016].

The aim of the master thesis is to study a novel process for *in situ* green synthesis of Ag NPs on cotton fibres, using $AgNO_3$ as a source of Ag and water extract of sumac leaf as reducing and stabilizing agent, without any additional chemicals. *Rhus spp.*, commonly known as sumac, is part of the family of *Anacardiaceae* which is comprehensive of more than 250 species, which composition and biological properties depend on the country of origin [Wang and Zhu, 2017], but generally sumac since antiquity has been used for food and for medical purpose against bacteria diseases and wound healing. Prior to the *in situ* synthesis of Ag NPs, the cotton fibres have been impregnated with an organic-inorganic hybrid sol-gel precursor to create a silica matrix on the surface of the fibres, reflecting in increased absorption of silver cations. Moreover, important aim was to study the influence of the concentration of the silver salt in the synthesis bath on the properties of the formed Ag NPs, whereas five different concentration of $AgNO_3$, i.e. 0.1; 0.5; 1.0; 2.5 and 5.0 %, were used. Accordingly, we assumed following:

- by the use of sumac water extract we will successfully formed Ag NPs on the surface of the cotton fibers;
- silica matrix will influence the increase of silver cations, leading to a higher concentration of Ag NP on cotton fibres and increase of the coating durability;
- increasing concentration of $AgNO_3$ in the synthesis bath will influence the Ag NPs size and their

concentration on the fibres;

- by increasing the concentration of Ag NPs on cotton fibres, functional antimicrobial and UV-protective properties of the modified fabric will increase; achieving sufficiently high initial concentration of Ag NPs on modified cotton fabric, we will create multifunctional protective coating with sufficient washing durability.

In order to confirm our assumption following analysis were obtained: scanning electron microscopy (SEM), energy dispersive X-ray spectroscopy (EDS) and inductively coupled plasma mass spectroscopy (ICP MS) to study morphological and chemical properties of the modified cotton fabric, bacterial reduction activity against Gram-positive (*Staphylococcus aureus*) and Gram-negative (*Escherichia coli*) bacteria to asses antimicrobial properties and UV-vis transmission and reflective properties to determine UV-protection. To study washing fastness of the coatings, the studied samples were repetitively washed once and five times. Their functional properties were assessed and compared to those obtained before washings.

CHAPTER 1

Theoretical background

Nanotechnology is a known field of research since last century and is raising interest for developing advanced functional materials at the nanoscale level in a wide range of field like drugs and medications, manufacturing and materials, environment, electronics, energy harvesting, mechanical industries [Khan et al., 2019]. Indeed, nanomaterials, which have at least one dimensions under 100 nm, are considered the bridge which fills the gap between bulk materials and atomic or molecular structures. Their dimensions and shape influence physical, chemical and biological properties, making them significantly different from the corresponding bulk materials due to their extremely large surface area to volume ratio. One of the main classifications that can be used is shape-based. Accordingly, nanomaterials can be insert in a ranking that includes 0D (quantum dots), 1D (nano rods, nanofibers), 2D (nano sheets), 3D (nanoparticles and nanowire networks) nanomaterials. This classification is dependent on the number of dimensions in the nanometre scale and consequently on the possibility of movement of surface electron. For example, electrons in 0D NMs are entrapped in a dimensionless space whereas as 1D NMs have electrons that can move along the x-axis, which is less than 100 nm. Likewise, 2D and 3D NMs have electron movement along the x–y-axis, and x, y, z-axis respectively [Jeevanandam et al., 2018]. Nanoparticles are classified as 3D materials which surface is estimated to be composed by 30-40 % of the total number of atoms composing the particle [Moreno-Garrido et al., 2015]. The particle itself can be schematized in 3 layers: the core, which is the central portion; the shell layer which is chemically different from the core and is responsible for the peculiar chemical and physical properties, and the surface layer, which may be functionalized with a variety of small molecules, metal ions, surfactants and polymers [Khan et al., 2019]. Changing the size, the shape, the crystallinity and the surface functionalization of NPs give tuneable physicochemical characteristics such as melting point, wettability, electrical and thermal conductivity, catalytic activity, light absorption and scattering resulting in enhanced performance over their bulk counterparts [Jeevanandam et al., 2018]. Currently nanoparticles can be organized into four material-based categories: carbon-based, inorganic-based, organic-based and composite-based nanomaterials. In the specific context of antimicrobial activity, main point of this research, inorganic synthetic nanoparticles seem to have been developed as one of the main gamers in the market. Both heavy metals, such as silver, gold, copper, titanium , zinc, and oxides, such as silver oxide (Ag_2O), titanium dioxide (TiO_2), copper oxide (CuO), zinc oxide (ZnO), calcium oxide (CaO) and magnesium oxide (MgO) have demonstrated antimicrobial activity against a wide spectrum of microorganisms. The toxicity and the modality of actions of these materials is still under assessment and is believed to be strictly dependent from shape, size, surface charge, composition and aggregation status of NPs. The toxic effect is also invariably dependant on the dose, route of administration and target [Fernando et al., 2018].

1.1 Silver nanoparticles

Among metal nanoparticles, silver nanoparticles (Ag NPs) is acquiring great importance in numerous applications in the market. Numerous researches indicate Ag NPs to have distinctive physio-chemical properties, including a high electrical and thermal conductivity, surface-enhanced Raman scattering, chemical stability, catalytic activity and non-linear optical behaviour. Besides, Ag NPs exhibit bactericidal, fungicidal, antiviral, anti-inflammatory, anti-angiogenic, anticancer activity [Zhang et al., 2016]. These properties lead Ag NPs to be applied in diagnostic, biosensor, and in gene therapy applications but also in cosmetic products, food storage, electronic components, environmental applications and textile coatings [Abbasi et al., 2016].

1.2 Anti-bacterial activity of Ag NPs

The Ag NPs have been demonstrated as an effective biocide against a broad-spectrum of bacteria including both Gram-negative and Gram-positive bacteria, in which there are many highly pathogenic bacterial strains [Tran et al., 2013]. Together with vaccine, antibiotics revolutionized medicine, but infections are becoming again one of the major causes of death throughout the developing world due to new infectious agents and more specifically due to the appearance of antimicrobial resistance. Indeed, in some part of the world antibiotics are prescribed too freely, resulting in resistance of bacteria to antimicrobial agents [Kapoor et al., 2017].

1.2.1 Gram-positive and Gram-negative cell wall

In order to better understand the antimicrobial activity of the nanoparticles, the detailed explanation about the compositional and structural features of the bacterial cell envelope and cell wall is compulsory [Kumar et al., 2017]. The typical bacterial outer surface is composed by three layers. The inner layer is a plasma membrane, composed by a phospholipid biolayer with some proteins gathered in between, which directs what enters and exits the cell. The cell wall, a structure that confers strengths and rigidity to the cell, determines bacterial cell morphology, prevents any mechanical damage, and protects the cell from rupturing due to turgor pressure developed inside the cell as a result of endosmosis [Kumar et al., 2017]. The cell wall is composed by peptide-polysaccharide layer called peptidoglycan or Murin, a heteropolymer composed by polysaccharide backbone of equal amounts of alternating N-Acetylmuramic acid (NAM) and N-acetylglucosamine (NAG) residues cross-linked through short peptide linkages [Kumar et al., 2017]. There is finally a sticky outer layer called capsule for protection and attachment. Based on composition, structure of bacterial cell wall and Gram staining characteristics, bacterial cells are classified into two main categories: Gram-positive (+) and Gram-negative (-) bacteria [Kumar et al., 2017].
Gram-positive bacteria present an inner plasma membrane called monoderm, composed by the double layer of lipids and several kinds of proteins that serve different functions. Follows the inner wall zone and a thick peptidoglycan cell wall, composed up to 30 layers. Another characteristic of the Gram-positive cell wall is the presence of lipoteichoic acids which anchor through the Murin to the lipids of the inner plasma layer. *Staphylococcus aureus* is the most common example of Gram-positive bacteria, which is part of the human microflora, especially present on the skin, but in its pathogenic form can be responsible of diseases, specifically some strains of *S. aureus* can cause intoxication and morbid manifestations of various types due to the secretion of exotoxin. Furthermore, it can be associated to the appearance of suppurative infections of the skin, the skeletal system, the respiratory tract, urinary tract and central nervous system. Among the others can be found *Bacillus anthracis*, responsible for anthrax, *Clostridium tetani* which is cause of tetanus, and *Streptococcus mutans* which is associated with cavities in the mouth.

Gram-negative bacteria present a more complex structure. The same plasma membrane as the Gram-positive bacteria compose the inner layer, but their cell wall is thinner, and anchored to an outer membrane of lipid biolayer with additional proteins. The outer plasma membrane presents proteins as well as the inner one, but among them appear porins which allow for passive diffusion the entrance of things from the outside in the periplasmic space between the two membranes, without any selection apart from size. The actual selective permeability of the cell is still controlled by the inner plasma membrane. Another very specific feature of Gram-negative bacteria is the presence of lipopoly-saccharides (LPS), at the very outside of the outer membrane, which bring to very important consequences in presence of infection of the blood, reason why are also called endotoxins. Namely the most common Gram-negative bacteria is *Escherichia coli*, which is part of the intestine flora of warm blood animals, but can be the main cause of intestinal and extra-intestinal diseases, such as urinary tract infections, meningitis, peritonitis, septicaemia and pneumonia. Some strains of *E. coli* are toxigenic, i.e. they produce toxins that can cause diarrhoea, especially as direct consequences of food poisoning. Other examples of Gram-negative bacteria: *Helicobacter pylori* which can cause ulcer and stomach cancer, *Vibrio cholerae* which is origin of cholera, *Yersinia pestis* responsible for plague and *Salmonella enterica* which is another common cause for food poisoning.
Both types of bacteria appear to be pathogenic, but the complexity of the structure is the reason why Gram-negative bacteria are usually more resistant to antibiotics, because of their impenetrable cell wall and fast ability to develop antibiotic resistance, even though an effect on the resistance of the bacteria is also given by the difference in thickness of the peptidoglycan layer that in Gram-negative bacteria is 5-10 nm [Kumar et al., 2017] while for Gram-positive is 20-30 nm [Feng et al., 2000].

1.2.2 Mechanism of antibacterial activity

The mechanism responsible for the bactericidal effect of Ag NPs has not been fully understood. Several experiments have been carried on to understand the bioactivity of the nanoparticles with the aim to solve one of the main elusive question that afflicts researcher from nearly a decade, whether the Ag NPs exert direct "particle-specific" effects beyond the antimicrobial activity of released silver ions (Ag^+) [Xiu et al., 2012]. The general effect can be summarized as follows: NPs in wet environment release silver ions; an initial attachment of Ag NPs or Ag^+ ions to the bacterial cell wall disturbs its proper functions, such as permeability and respiration, leading to the disruption of the membrane and the leakage of cytoplasmic content, with subsequent penetration of ions inside the cell, ROS and free radical generation, disruption of ATP production and DNA replication, protein denaturation, and eventually the death or the inhibition of the cell.

Plasma membrane disruption through Ag NPs interactions

Hypothetical mechanisms of action include the direct interference of clumps of nano silver that settle on the surface of cells, attracted by electrostatic attraction, van der Waals forces, and receptor–ligand. Both Gram-negative and Gram-positive bacteria at biological pH exhibit a negative surface charge because carboxylic acid groups in the surface proteins and become sites of metal cation attraction. This negative charge does not appear distribute uniformly all over the bacteria surface but organized instead in anionic surface domains, which leads to a greater focal toxicity for higher NPs concentration in these areas [Slavin et al., 2017]. Nanoparticles with size greater than 10 nm are adsorbed on the outer surfaces of the bacteria, neutralising the surface potential of the membrane which results in increased surface tension and membrane depolarization. Follows a general disorganization of the cell wall that slow down bacteria growth: there is a change in membrane texture, induction of oxidative stress and an increasing membrane permeability compromises cell membrane integrity and allows a greater influx of metal ions and NPs in the cytoplasm, with consequent leaks of intracellular fluid

and components (cellular factors, LPS and membrane proteins). The accumulation of Ag NPs and Ag^+ on the surface of the bacteria cell brings to electrostatic imbalance and consequent dissipation of the proton promotive force for ATP synthesis, thus disrupting the chemiosmotic potential of the membrane and causing leakage of intracellular K^+, depleting almost the entire cell's supply of K^+ [Slavin et al., 2017]. Creation of pits due to lipids destruction, modification of the bacteria morphology and ultimate rupture of the membrane lead to bacterial cell death [Slavin et al., 2017], as reported by several microscopic techniques used to uncover changes in structural/mechanical properties of the bacteria cell wall surface upon Ag NPs exposure [Slavin et al., 2017]. The cell wall destruction that occurs from physical interaction between NPs and the cell wall is more detrimental for Gram-negative bacteria as they lack the thick peptidoglycan layer found in Gram-positive bacteria that could possibly act as a protective layer. Another potential reason for Gram-negative susceptibility to NPs is that Gram-negative bacteria are coated with lipopoly-saccharide molecules in the outer leaflet of the lipid bilayer, which have more charge per unit surface than other phospholipids and hence the electrostatic interaction leading to a buildup and increased uptake of ions [Slavin et al., 2017].
Furthermore, should not be neglected the possible effect of abrasion from corners, edges, or defects in nanoparticles that creating physical damages the cell wall contributes to its lysis [Raghunath and Perumal, 2017].

Cellular internalization of Ag NPs

Porins on the membrane, which are in the micrometre range, and progressive permeability of the membrane, bring nanoparticles which size is inferior to 10 nm to penetrate in the cytoplasm, as reported by several research [Martinez-Castanon et al., 2008, Liao et al., 2019, Agnihotri et al., 2014]. Has been observed that the nanoparticles gathering along the metabolic pathway were able to influence the shape and function of the cell membrane like permeability and respiration. Thereafter, NPs bind with mesosomes and alter cellular respiration, bring oxidative stress, electrolyte balance disorders, enzyme inhibition, protein deactivation, and changes in gene expression. Nevertheless, is believed that silver nanoparticles exert their bactericidal activity through a Trojan-horse mechanism, since after cell-barrier penetration they promotes the release of silver ions, thereby enhancing the amount of cellular uptake of particle-associated Ag^+ ions and promoting redox cycle in the cytosol and intracellular radical accumulation [Tomsic et al., 2008].

Metal ions release

Is well known that silver nanoparticles can be oxidized in aqueous solutions exposed to air (Equation 1.1) resulting in the release of silver ions under acidic conditions (Equation 1.2).

$$4\,Ag^0 + O_2 \longrightarrow 2\,Ag_2O \tag{1.1}$$

$$2\,Ag_2O + 4\,H^+ \longrightarrow 4\,Ag^+ + 2\,H_2O \tag{1.2}$$

Appear evident from the shown equation that in anaerobic environment, very little Ag^+ ions are released, resulting in low toxicity the NPs [Liao et al., 2019]. The metal ions release can be highly affected by the presence of bacteria, which depending on their metabolic state could influence the dissolved oxygen concentration (Equation 1.1), pH (Equation 1.2), release or remove the coating of Ag NPs and, by binding the released Ag^+, increase the silver dissolution gradient [Lok et al., 2007]. Also the contamination by ligands such as chloride, sulphide, phosphate or organic acid in the aqueous medium of exposure can affect the effectiveness of the agents, indeed, binding the released ions the bioavailability of Ag^+ is decreased [Martinez-Castanon et al., 2008]. Moreover, it has been reported that presence of UV irradiation accelarate release of ions, ascribed to photooxidation reactions [Zhang et al., 2015]. Ag NPs contain free electrons, that can interact strongly with light by either absorbing or scattering the photons. When NPs are excited by light of wavelength longer than the size

of the NPs, the oscillating electric field of the incoming radiation induces coherent collective oscillation of the free electrons (conduction band electrons) on the metal surface. When the frequency of the incident light photons equals the oscillating frequency of electrons, a resonance phenomenon, called localized surface plasmon resonance (LSPR), occurs [Zhang et al., 2015]. The energy is absorbed and generates electron-electron scattering and electron-phonon coupling. The created hot electrons have high energy and may be ejected to leave the nanoparticle positively charged and break up to form smaller particles if sufficient charge is accumulated [Cheng et al., 2011]. Silver ions, leached from NPs and dispersed in the surrounding medium, carry a positive charge, bringing electrostatic interaction into play. Attracted by the negative charge of the bacteria cell wall previously discussed, they can be adsorbed on the bacteria surface, interacting with the carboxyl and thiol groups of cell-wall-bound enzymes and proteins, or penetrate the cell wall into the cytoplasm, in a process known as biosorption. Metal ions block respiration and neutralise the charges on LPS increasing the permeability of the outer membrane contributing to the accumulation of nanoparticles or ions inside the cell slowly leading to the cell wall destruction [Raghunath and Perumal, 2017]. Through transmission electron microscopy imaging has been possible to observe and prove interaction among silver cations and cell surface component. Indeed, cell of both *E. coli* and *S.aureus* treated with silver cation shown a physical separation between the cell wall and the internal cellular environment. Moreover, surrounding the lysed cell an electron dense aggregation of compounds has been observed, result of the interaction between Ag^+ with negatively charged compounds located in the bacterial cell wall such as phosphate, carboxyl, and amino groups that caused Ag precipitation [Slavin et al., 2017]. Ag^+ catalyse the oxidation of amino acid side chains resulting in protein-bound carbonyls which leads to loss of catalytic activity in the case of enzymes, ultimately triggering protein degradation. In addition, these ions react with the functional groups such as mercapto (–SH), amino (–NH), and carboxyl (–COOH) of many proteins essential to the ATP production and nucleic acid, inactivating their activity [Wang et al., 2017]. Metal ions bind with DNA and disrupt the helical nature by cross-linking between and within DNA strands, due to their reactivity in presence of phosphorus [Raghunath and Perumal, 2017]. Consequently, DNA loses its replication ability.

ROS formation

The ROS (reactive oxygen species) are all the molecules and reactive intermediates that have strong positive redox potential: the four types are the superoxide radical (O^{2-}), the hydroxyl radical (HO•), hydrogen peroxide (H_2O_2), and singlet oxygen (O_2), which exhibit different levels of dynamics and activity [Wang et al., 2017]. Under normal circumstances, the production and clearance of ROS in bacterial cells are balanced, because they're generated through aerobic pathways in electron transport chains during bio-redox reactions, but bacteria cells protect themselves from ROS damage through the use of enzymes such as superoxide dismutases (SOD, to convert superoxide to hydrogen peroxide) and catalases (to convert hydrogen peroxide to water and oxygen) [Choi and Hu, 2008]. Nevertheless, ROS production can increase, leading to cell damage or cell death, if the bacteria is subjected to external stress [Slavin et al., 2017]. Ag NPs have been shown to enable the production of reactive free radicals [He et al., 2014] through two main and coexisting mechanism: Fenton-like reaction and surface plasmon resonance enhancement.

Fenton-like reaction. Fenton reaction is the process of production of hydroxyl radicals due to the reaction between H_2O_2 and transition metal ions (Equation 1.3), or zero valent metal NPs (Equation 1.4) when their redox potential is lower than the one of H_2O_2/H_2O (1.77 V) as in the case of elemental silver (Ag^+/Ag 0.7996 V).

$$H_2O_2 + M^{n+} \longrightarrow M^{n+1} + HO^- + HO\bullet \tag{1.3}$$

$$M(NP) + H_2O_2 + nH^+ \longrightarrow M^{n+} + H_2O + HO\bullet \tag{1.4}$$

Fenton reaction leads to the progressive silver cations production and ROS creation in a mechanism that seems to be strictly interlaced [He et al., 2014]. Nevertheless the presence of this reaction has still to be confirmed since it has been proved that no ROS generation appear in absence of light. The main production of ROS seems to be attribute to photocatalytic effect of Ag NPs as following described [Choi and Hu, 2008].

Local surface plasmon resonance enhancement. LSPR mentioned in the previous paragraph, induces a strong absorption of the incident photon energy, which can be transferred to O_2 and lead to $^1O_2$ generation. The photoelectrons transferred to O_2 are responsible for the generation of O^{2-}, which can further promote the generation of HO• under UV irradiation, reacting with H_2O_2 according to Haber-Weiss cycle reaction (Equation 1.5 - 1.6) [Zhang et al., 2015].

$$HO\bullet + H_2O_2 \longrightarrow H_2O + {O_2}^{2-} + H^+ \tag{1.5}$$

$${O_2}^{2-} + H^+ + H_2O_2 \longrightarrow O_2 + HO\bullet + H_2O \tag{1.6}$$

Plasmon resonance can be affected from the size, shape, dielectric environment, and mutual electromagnetic interactions among particles. These parameters can be used to tune the plasmon peak of Ag NPs in the range of 393–738 nm and 500–1000 nm [Wei et al., 2015]. Unlike semiconductors, metallic and single-element NPs have fundamentally different electronic structures that have not been explicitly correlated with ROS generation [Zhang et al., 2015]. Such knowledge is of considerable practical significance, because attempts to inhibit or enhance ROS-induced pathology are most likely to succeed by manipulating the extent of damage to the bacteria [Du and Gebicki, 2004].
ROS production primarily affects respiratory enzymes. Highly reactive, but short-lived HO• will non-selectively oxidize all types of macromolecules such as lipid, polysaccharide, protein and DNA. Superoxide radical O^{2-} generates damages to iron–sulphur (Fe–S) clusters in the electron transport chain, releasing more ferrous ions thus decreasing ATP production. These ferrous ions are oxidised by the Fenton reaction, generating more HO• and eventually damaging DNA, proteins and lipids. However, O^{2-} dismutation reactions produce hydrogen peroxide (H_2O_2), and the reaction among these two radicals can lead to HO• and $^1O_2$ production [Zhang et al., 2015]. Rather long-lived $^1O_2$ can react with unsaturated fatty acids, beta-carotene, amino acids and methionine [Zhang et al., 2015]. Furthermore, the action of silver ions, which interacts with glutathione, a non-enzymatic antioxidant, lead to an excessive generation of ROS within the bacterial cell. Oxidised glutathione increases lipid peroxidation in the bacterial membrane leading more peroxyl radical intermediates and causing alterations in membrane fluidity and integrity [Raghunath and Perumal, 2017].

Toxicity concern of Ag NPs Ag NPs incorporation in cosmetics, food packaging, textile coating, but also water and air filters arise the concern about exposure to NPs by dermal contact, oral administration, inhalation, and blood circulation, and subsequently to possible interaction with the living organism. Nonetheless, the mechanisms of toxicity in humans still remain largely uncharted. The very first known effect is argyria, a permanent bluish-grey discoloration change in colour of eyes and skin. Besides these discolorations, exposure to soluble silver may produce damage to liver and kidney, irritation of the eyes, skin and respiratory tract. In vitro experiments showed toxicity on macrophages, first line on defence of human body, with evident size dependent results [Pratsinis et al., 2013]. Other cell line tested, murine fibroblast and keratinocyte resulted actually more sensible to Ag NPs contact which induced effects on cellular metabolic activity and membrane damage as most pronounced. Indeed, there is evidence that shows that silver ions cause changes in the permeability of the cell

membrane to potassium and sodium ions at concentrations that do not even limit sodium, potassium, ATP, or mitochondrial activity [Prabhu and Poulose, 2012]. Moreover, mouse germ line stem cells and rat cells derived from skin, liver, lung, brain, vascular system and reproductive organs resulted damaged even from low-level and short -time exposure to silver nanoparticles resulting in oxidative stress and impaired mitochondrial function [Prabhu and Poulose, 2012].
In vivo experiment where performed on mice and rats subjecting them to oral administration, inhalation and intraperitoneal injection of different size and doses of Ag NPs. Subsequently to exposure the nanoparticles were detected in several organs including liver and brain. Accumulation in other organs was negligible but damages to respiratory tract was reported, with influence on neutral mucins in the respiratory mucosa. It was also found from histopathological studies that there was a higher incidence of bile duct hyperplasia, with or without necrosis, fibrosis, and pigmentation in the study animals. In vivo sedimentation reported lower toxicity than in vitro ones [Prabhu and Poulose, 2012, Wei et al., 2015, Epstein et al., 2014]. Difference in results in the tested animals resulted from difference in sex, resulting in a predisposition in female gender to silver accumulation in the organism. However, data on absorption and internal systemic exposure of nanomaterials is limited and may vary depending on local barriers present in different organs and from physicochemical properties of the individual particles, which makes the concentration-dependent toxicity issue pointless if not considered together with comparison in term of size shape and chemicals bonded to the NPs surface.

Concerns around the contact of silver NPs through clothes and wound dressing for prevention of sepsis of skin wounds like burns and ulcers have been investigated. Nanoparticles are bonded to textile fibres only by physical forces and repetitive friction, sweat and other body excretions can accelerate the process of leaching of the antimicrobial compounds [Simoncic and Tomsic, 2017]. Several studies have reported transdermal penetration of nanoparticles with the possibility for the particle to be phagocytized by macrophages and Langerhans cells and consequent perturbations of the immune system. Therefore, skin sensitization is a highly relevant parameter when evaluating the hazardous effects of active antimicrobial compounds. The uptake of nanomaterials is generally considered to be very low to absent, even when epithelial tissue appears damaged. The Danish EPA analysed various textile products containing (nano-)silver in contact with artificial saliva, sweat or waste water. The released of particles varied significantly between various fabrics (0.02-84%) but very little biological risk was assessed. Further assessment conducted from Von Götz et al. revealed that dermal exposure from NPs from coated textile is not a worthy pathway for future research in comparison to other form of possible exposure route [Epstein et al., 2014]. Also research in medical field, in which contact with skin may allow nanoparticles to penetrate through compromised barrier and gain access to the dermal capillaries, revealed that after treatment of burn wounds with silver impregnated product silver nanoparticle were found both in blood stream and urine, suggesting systemic availability and urinary excretion of the Ag originating from the wound dressing. Investigation on the usage of silver coating in textile seems to bring greater benefits of the disadvantages that can derive from possible contact, also considering that the amount of the released Ag from textiles in immediate surroundings directly depends on its concentration on the fibres and the pH of the surrounding area. At pH 5.5, which is near the pH of healthy skin, the concentration of the released silver was determined to be the lowest [Simoncic and Tomsic, 2017].

1.2.3 Influences on Ag NPs antibacterial activity

Particle properties such as size, shape, surface coating and surface charge likely affect toxicity indirectly through mechanisms that influence the rate, extent, location, and/or timing of Ag+ release and ROS formation [Xiu et al., 2012].

Size

Most of the researchers agree in stating that a smaller dimension of nanoparticle enhance its antibacterial activity. Indeed the reduction of size affects surface area-volume ratio and surface reactivity [Akter et al., 2018]. Larger specific surface area results in higher probability of being in touch with the bacterial cell membrane [Wang et al., 2017] and bring to higher release of metal ions and a greater production of ROS, which consequently can damage and inactivate essential biomolecules, including DNA, proteins, and lipids [Slavin et al., 2017]. Has been verified that 7 nm silver nanoparticles present better antibacterial against *E. coli* and *S. aureus* in comparison to 29 nm or 89 nm spherical NPs [Martinez-Castanon et al., 2008]. Has not to be neglected that nanoparticles which size is inferior to 10 nm can easily reach the nuclear content of bacteria passing through porins of bacterial cell wall [Martinez-Castanon et al., 2008]. This results as a direct influence on the MIC requested for antimicrobial activity: smaller NPs will perform the same activity of a lager load of larger NPs [Simoncic and Klemencic, 2015]. Moreover, sedimentation velocity, mass diffusivity, attachment efficiency, and deposition velocity of NPs over the biological or solid surfaces are considerably influenced by particle size. Thus, the size effect is not the dominant factor.

Shape

Ag NPs can be produced in different shapes depending upon synthesized conditions [Liao et al., 2019]. Among the known shape that has been produced in recent years we can find planar (triangles, 5 or 6 diagonal, round surfaces, etc.) and three dimensional (cubic, pyramid, etc.) NPs, apart from spherical nanoparticles that are the most thermodynamically stable [Khodashenas and Ghorbani, 2015]. The main reason for shape-dependency effectiveness is the different specific surface area and facet reactivity of crystal plane. The high atom density {111} plane appear to be the most reactive and therefore the most susceptible to the process of oxidation. ROS formation is also dependent from morphology since molecular (O_2) form singlet $^1O_2$ only on the Ag(111) surface, but dissociates into an atomic form on both Ag(100) and Ag(110). Therefore, singlet $^1O_2$ can only be photo-sensitized and formed on Ag nanostructures having the Ag(111) surface, such as Ag decahedrons and Ag triangular plates, but not (or very minor) on the Ag nanostructures having the Ag(100) surface, such as obtuse Ag nanocubes. Different investigation conducted both on Gram-positive and Gram-negative bacteria reported without contrast a major efficiency in antibacterial activity of cubic and truncated triangular shape over spherical shape, wire and rod shaped NPs.

Capping agents

During NPs production, to avoid agglomeration, a number of capping agents can be used, each of them leading to specific effect on the hydro-radius of the nanoparticles that will differ from the proper dimension of the produced particle bringing both to sterical repulsion between NPs, and electrostatic interaction. Indeed, agglomeration would diminish the size dependence bioactivity, reducing the ratio surface to volume. But one of the main points of the capping agent in antimicrobial activity is to impart an electrostatic charge to the surface in order to enhance the interaction with the bacteria. As aforementioned, both Gram-positive and Gram-negative bacteria bring on their surface a negative charge. Capping agent able to confer a surface positive charge to nanoparticle would exert a better adhesion and adsorption to the bacteria cell wall. Among the main capping agent that can be applied in Ag NPs production PVP, citrate (CT) and branched polyethyleneimine (BPEI) can be found. The BPEI-Ag NPs are electro-sterically stabilized through adsorption of the BPEI polyelectrolyte containing amine groups, which ionize in the solution to create charged polymers. Investigation on the efficacy of the major capping agents led to the measurement of zeta potential which resulted in -38 mV in CT-Ag NPs, -10 mV for the NPs coated in PVP and 40 mV for BPEI-Ag NPs. Verified antibacterial activity accordingly was higher for positive charged nanoparticles, indeed BPEI-Ag NPs

interact strongly with the negatively charged moieties in the bacteria membrane [Liao et al., 2019]. Similarly, PEI Ag NPs, where PEI is a cationic polymer in which the amino groups provide Ag NPs with a positive charge, reported a zeta potential of 49 mV. Its bactericidal activity resulted high against a broad spectrum of Gram-positive (*S. aureus*, *Streptococcus mutants*, and *Streptococcus pyogenes*) and Gram-negative bacteria (*E. coli* and *Proteus vulgaris*) [Liao et al., 2019]. However, due to a wide spectrum of antimicrobial activity it seems interesting to continue the study in order to find factors which can maintain antimicrobial activity of the NPs, minimizing the possible cytotoxicity, for example, chitosan-derived polysaccharide-coated Ag-NPs showed antimicrobial activity with no toxicity to eukaryotic cells. On the other hand, the use of capping agent changes the diffusion coefficient of the nanoparticles affecting their mobility through bacterial growth medium, cell membrane and cytoplasm. Total capping can lead to a significant decrease of antibacterial effectiveness limiting the contact between silver surface and bacteria cell wall.

Environment

Nevertheless, capping agents can change their effectiveness according to the environmental condition such as pH and osmotic pressure that can lead to a change in their sterical radius or surface charge. Temperature of the environment can also lead to change in the rate of dissolution of silver cations and ROS generation. Other studies propose an oxidative dissolution mechanism for Ag NPs through the interaction of Ag^+ with dissolved oxygen and protons. Diversification in aquatic chemistry could activate Ag NPs, enhancing the antibacterial activity of the Ag NPs due to the release of Ag ions, that as showed in Equation 1.2 is higher in acidic environment [Slavin et al., 2017]. As aforementioned also condition of aerobic and anaerobic environment strongly affect the chemical reaction involved in antibacterial activity as much as the presence of UV radiation [Slavin et al., 2017].

1.3 Production of Ag NPs

Production of silver nanoparticle can be performed following several path considering the importance of the cost and the scalability of production, that doesn't have to affect the quality of the NPs in term of particle size, dispersion and purity. For application on textile, there are two possible way of action: incorporation of pre-produced silver nanoparticles or *in situ* synthesis. Silver nanomaterials can be obtained by both the so-called "top-down" and "bottom-up" methods. The top-down method involves physical methods such as milling or attrition, repeated quenching and photolithography [Epstein et al., 2014]. Nevertheless, obtaining NPs from bulk metals and subsequent stabilization of the resulting nanosized metal particles by the addition of colloidal protecting agents [Prabhu and Poulose, 2012] is not usually the most used technique since it has the higher cost in term of quality loss of the final product. Indeed, usually these techniques never present an homogeneous grinding of the material presenting high dispersion in size. Furthermore, the particle before use have to be dispersed in an appropriate solvent, but even with ultrasound pre-treatment, a good suspension is impossible to achieve due to strong aggregation of nanoparticles. Accordingly, application on textile has to be performed under continuous stirring [Tomsic et al., 2008]. The bottom-up methods, according to literature include conventional and unconventional methods. Conventional synthesis methods include the use of citrate, borohydride, two-phase (water-organic) systems, organic reducers, and inverse micelles in the synthesis process. Unconventional methods include laser ablation, radiocatalysis, vacuum evaporation of metal, and the Svedberg method of electrocondensation [Epstein et al., 2014]. Each method of production gives a different possibility to tune particle size and shape as well as functionalize the nanosilver with capping agents that makes it suitable for specific applications. Although chemical and physical approaches have the high ability to shape-controlled synthesis of nanoparticles, they have some drawbacks using toxic chemicals in the synthesis process and the high cost of energy

and equipment. These are the main reason for increasing effort of the researchers to develop process for green synthesis of Ag NPs. Such green synthesis includes the use of naturally derived reducing and stabilizing agents, like plants (i.e. bark,branches, roots, leaves, seeds and fruits) extract, in no toxic solvents, i.e. water or alcohol. Results achieved so far are encouraging for operational simplicity, high yield, matching less generation of toxic substances. Nevertheless, cubic or spherical nanoparticles can be produced either following physical, chemical or biological methods, but for synthesis of other shapes (nanorods, nanowires, and nanobars) due to the underdevelopment of biological methods, using either chemical or physical methods is inevitable [Khodashenas and Ghorbani, 2015].

1.3.1 Wet Chemical Route

The chemical route is the cost-effective and allow great productivity and reproducibility. Moreover, is possible with the same chemicals to produce nanoparticles with different size and shape, leading to products with completely different characteristics. Main limitation appears to be use of toxic agent in precipitations and lack of purity in the final product. The ease of the chemical reduction is given from the use of only three components: metal precursors, reducing agents, stabilizing and capping agents. The reaction can be carried out in aqueous or non-aqueous solutions. The formation of nanoparticles in colloidal solution is divided in three steps. The reduction involves a first step of dissolution of the salt in a solvent, consequently, with the action of the reducing agent, nucleation begin: Ag^+ to Ag^0 atoms, and subsequent aggregation of Ag^0 atoms to form clusters, $(Ag^0)_n$, according to the reactions: $nAg^+ \longrightarrow nAg^0 \longrightarrow (Ag^0)_n$, or via a step wise reduction mechanism: $Ag^+ \longrightarrow Ag^0 \longrightarrow {Ag_2}^+ \longrightarrow {Ag_4}^+ \longrightarrow \ldots \longrightarrow (Ag^0)_n$ [Liao et al., 2019]. When the critical size is reached, is possible to have the growth of the nanoparticles. Shape and size are strongly dependent from the developing of these two stages, as much as the monodispersion of size. As far as the use of silver salt, silver nitrate ($AgNO_3$) is extensively used for silver production because of its chemical stability and low cost compared to other silver salts. Typical reductants are sodium borohydride ($NaBH_4$), ascorbic acid, glucose, hydrazine, sodium citrate, and ethylene glycol (EG). According to studies, while the first is a very strong reductants for silver salts, which leads to fine and monodisperse NPs, the others gives less fine product. If $NaBH_4$ is used in stochiometric excess in the reaction with silver salt, BH_4^- anions can dispose on the surface of the formed NPs and act as stabilizing agent [Simoncic and Klemencic, 2015]. Stabilizing agent has a strong effect on growth and shape of the nanoparticles, reduce agglomeration, prevent precipitation and sedimentation keeping stable the colloidal silver. Electrostatic or steric stabilization of colloidal Ag NPs is achieved through adsorption of macromolecules or organic compounds to the surfaces of the nanoparticles. Typical polymer-based capping agents are polyvinyl alcohol (PVA), polyvinylpyrrolidone (PVP), polyethylene glycol (PEG) and polysaccharides, while non-ionic surfactants including Brij, Tween, and Triton X-100 are employed to stabilize Ag NPs during the formation process. Sodium citrate is also used as capping agent because of its carboxylic moiety which exhibit negative charge [Liao et al., 2019]. Furthermore, has been investigated the possibility to use seed particles during the reaction process to enforce a stronger influence on the particles morphology [Liao et al., 2019]. Among the most used techniques of Ag NPs production the polyol process is the most used. The polyol process is based on the decomposition of a polyol (EG in most of the cases found in literature) at an elevated temperature, typically 160°C, followed by reduction of the metal ions to their elemental states, with possible presence of a surfactant (usually PVP). The reduction, in case of ethylene glycol follows the mechanism reported in Equation 1.7 and 1.8.

$$2\,HOCH_2CH_2OH \longrightarrow 2\,CH_3CHO + 2\,H_2O \tag{1.7}$$

$$2\,Ag^+ + 2\,CH_3CHO \longrightarrow CH_3COCH_3CO + 2\,Ag + 2\,H^+ \tag{1.8}$$

Thermal heating is usually applied to rule the temperature process but recently a microwave assisted method has been developed since has been proved to offer fast and homogeneous heating of the reaction medium, typically in a time period of few seconds. This affects the reaction providing uniform nucleation and growth conditions for Ag NPs [Liu et al., 2006]. Ethylene glycol can serve both as reductant and as solvent and the presence of PVP can play an important role in tuning size and shape of the NPs constraining the growth of distinct crystal faces. For example, taking advantage of the selectively adsorption on the {1 0 0} facets, silver nanosphere has been produced in absence or using low amount of PVP, while uniform silver nanowires were the typical shape with the use of low molecular weight of PVP [Martinez-Castanon et al., 2008]. Polyol process can also be influenced by the application of different way of addition of the precursor: NPs of small size, in the range of 20 m, with narrow distribution have been successfully produced by injecting a modified precursor in the solution, obtaining rapid nucleation in a short period of time [Martinez-Castanon et al., 2008]. In this method, precursor injection rate and *in situ* conditions (inside the reaction mixture) acted as governing factors [Haider and Kang, 2015]. Modulating the chemical and redox environment by temperature, pH, surfactants, metal ions, eventual dopant or seeds concentration drastic effects on the shape and size of the product that can be obtained.

Microemulsion is also another typical synthesis route used to tune fine size and size dispersion. This technique as well as chemical reduction involves three main factors: water, oil and one or more surfactant agents. Depending on the proportion of various components and hydrophilic–lipophilic balance (HLB) value of the surfactant used, the microdroplets in the microemulsion can be in the form of oil-swollen micelles dispersed in aqueous phase as O/W microemulsion or water-swollen micelles dispersed in oil phase as W/O microemulsion [Zhang et al., 2007]. This second system is the typical one used for NPs production. Microdroplets of water disperse in a continuous oil phase act as microreactor for the reduction. Usually two microemulsions are prepared, one of them carrying silver precursor, while the other one carrying the reducing agent. The two microemulsions are then mixed leading to the collision and coalescence of water micelles. After diffusion and exchange of reactants among the different micelles, nucleation begins. The growth of silver goes on till attain the dimension of the water pool. At the end of this step surfactants, that were used to contain water, attach to silver surface preventing further aggregation. Silver nitrate is used as a precursor while among the typical surfactants we can find cationic surfactants such as cetyltrimethylammonium bromide (CTAB), anionic surfactants such as bis(2-ethylhexyl)sulfosuccinate (AOT), sodium dodecyl benzene sulfonate (SDBS) and lauryl sodium sulfate (SDS), and nonionic surfactants such as Triton X-100. The droplet dimension can be modulated by various parameters, the surfactants among the others and water-to-surfactant molar ratio. obviously that the particle size increases with the water content (W) and it has also been noticed that there is a decrease in the size distribution at low W compared to that of the particles obtained with higher W [Zhang et al., 2007].

Among the other techniques used to ease the chemical reduction of silver salt, photoreduction can be performed, and researchers indicated successful results deriving from the use different light sources (UV, white, blue, cyan, green and orange) at room temperature showing great versatility. Ag NPs are synthesized by photoreduction of precursor or Ag ions using photochemically activated intermediates such as radicals[Haider and Kang, 2015]. Sodium nitrate, Triton X-100 and carboxymethylated chitosan have been reported already for traditional chemical reduction, used both under the role of reducing agent and NPs stabilizers, leading to size of nanoparticles under 10 nm, stable in aqueous suspension [Haider and Kang, 2015, Tran et al., 2013].

Nevertheless as aforementioned the chemicals implied in the production of NPs are toxic and hazardous for the environment, and do not guarantee good properties of the product, since they

sediment on NPs surface, leading to possible unwanted and dangerous contamination in their possible use [Zhang et al., 2016].

1.3.2 Physical Route

Among the most quoted physical method the process of evaporation- condensation, using a tube furnace at atmospheric pressure. The process consists in a evaporation of a silver wire in a tungsten boat in the middle of a furnace. A carrier gas cool down the vapour of the metal and the atoms form nuclei due to a large degree of supersaturation. After nucleation, particle growth occurs by coagulation and subsequent coalescence of nuclei in the hot growth region above the evaporation source. This method present numerous drawbacks: indeed, the machinery itself obliges to deal with great quantity of energy and requires a lot of time to achieve thermal stability [Liao et al., 2019, Baker et al., 2005].
Furthermore, silver nanoparticles have been synthesized with laser ablation of a metal silver plate in an aqueous solution of sodium dodecyl sulfate (SDS). The metal plate placed on the bottom of a glass vessel filled with a aqueous solution of SDS, was irradiated by the focused laser (532 nm). Upon irradiation of the laser beam, the solution gradually turns brownish-yellow due to the formation of NPs with diameter lower than (10 nm). One advantage of laser ablation compared to other conventional method for preparing metal colloids is the absence of chemical reagents in solutions [Mafune et al., 2000].
Physical route has a distinct advantage in forming high-purity Ag NPs. However, it is a low yield process, which often requires high temperature and power consumption with high cost of investment for the basic equipment. In addition, the lack of surface functionalization, which can be useful for further application, makes difficult the dispersion in solvent and lead to agglomeration.

1.3.3 Biological Synthesis

Traditional routes of nanoparticle productions often require high pressure, energy, temperature and toxic chemicals as previously described. Nevertheless, one cannot deny their growing applications in daily life. Especially silver nanoparticles that are striving towards the edge-level utilities in every aspect of science and technology cannot be neglected just because of their source of generation [Ahmed et al., 2016]. Green synthesis is acquiring more and more interest in the last decades for using environmentally benign processes, taking advantage of the potential renewable feedstock coming from nature [Rayne and Mazza, 2007]. Natural biomolecules such as microorganism, enzymes, and plants or plant extracts are being studied as reducing and stabilizing agents in the nanoparticle production, increasing their application in functional modification of textiles. Furthermore, biosynthesis routes appear to be faster, cost- effective and more suitable for up scaling synthesis of nanoparticles [Baghizadeh et al., 2015] especially considering plants instead of microorganism for the employment of less resources for cell culture maintaining. Phytochemical analysis of plant extract of leaves, roots, shells, seeds and stems usually results in showing the presence of alkaloids, steroids, terpenoids, phenolics, flavonoids, tannins, high-low molecular weight proteins and saponins and these compounds because of the presence of hydroxyl (–OH), carboxylic (–COOH), amino ($–NH_2$), or thiol (–SH) groups, offer reduction and stabilizing capacities for NPs in a complex redox mediated process [Jha and Prasad, 2016]. Furthermore, they are known to exhibit the physiological activities and medicinal properties in plants, which can add further advantages for final purposes of NP, especially in sanitary or medical application [Jha and Prasad, 2016]. However, identification of medicinally active phytochemicals is a time-consuming, challenging, and complex procedure due to several complexities in the identification of the exact chemical components responsible for the synthesis and stabilization of metallic nanoparticles, and there is lack of comprehensive reviews that presents mechanistic aspects of biosynthetic pathways of NP synthesis [Ovais et al., 2018].
Silver nanoparticles have been synthesized using various types of plants, including *Gossypium hirsutum* [Vanti et al., 2018], red sanders powder extract [Rao et al., 2019], *Cuminum Cyminum* leaf

extract [Karamian and Kamalnejad, 2019], pomegranate peel extract [ul Islam et al., 2019], *Curcuma longa* tuber powder and extract [Muthuswamy Sathishkumar, 2010], *Stachys lavandulifolia* extract [Shahriari et al., 2017], Prunus japonica leaf extract [Saravanakumar et al., 2016], *Aloe vera* leaf extrac [Zhou et al., 2017], *Seidlitzia rosmarinus* ashes [Aladpoosh et al., 2014], *Allium cepa L.* extract [Sharma et al., 2017], *Eucalyptus citriodora* and *Ficus bengalensis* leaf extract [Ravindra et al., 2010]. The developed silver nanoparticles by this process have excellent properties, including long term dispersion stability [Ravindra et al., 2010]. The huge pool of bioresources from plants and microbes, if rightly utilized, could enable biosynthesized nanoparticles to turn into a game changer in the near future. Thus, there is a tension in the use of agriculturally optimum land worldwide for producing biologically sourced industrial and health-based chemicals, versus the production of food product for human consumption [Rayne and Mazza, 2007]. For this reason, efforts are underway to identify and investigate potential industrially valuable crops rich in bioactive components that can grow in marginal lands with little or no fertilizer or irrigation inputs [Rayne and Mazza, 2007].

Sumac

In this study, sumac leaves extract was used both as a reducing and stabilizing agent for antimicrobial finishing of cotton via facile and rapid *in situ* biosynthesis of Ag NPs. To the best of our knowledge, the production of the micro- and nanoparticles of metals or metal oxide has never been performed using any of the sumac plant parts as phytochemical. Sumac, common name for the *Rhus genus* in the family of the *Anacardiaceae*, is a shrub or a small tree that can reach 5–10 m in height. Its leaves are oddly pinnate (feather-like) and the plant flowers from May to July and the fruits may ripen from June to September in the northern Hemisphere. The ripened fruits of sumac present dense conical clusters of small compact reddish drupes [Wang and Zhu, 2017]. The genus contains over 250 individual species, naming among the most representatives *R. coriaria* (tanner's sumac), *R. copallina* (winged or shining sumac), *R. glabra* (smooth sumac), *R. undulate* (Kuni bush), and *R. verniciflua* (Japanese sumac), which are native to Mediterranean Basin, Eastern North America, Western North America, South Africa and Asia, respectively [Wang and Zhu, 2017]. Because of its ecological benefits, horticultural uses and brightly coloured foliage during fall it has been introduced for soil conservation, sand stabilization and urban forestation in many other countries and now is widely spread worldwide [Zhang et al., 2009]. Indeed, this fast-growing species compete aggressively for soil resources with the autochthonous flora, becoming invasive into its non-native habitats. It can not only grow under environmental stresses, such as drought, low temperature, low soil nutrient environments and low light but is also highly effective in retaining water and soil due to its colony-forming growing pattern [Zhang et al., 2009]. Its competitive behaviour allows the plant to grow in marginal regions without creating competition with crops reserved for food production. This feature appears relevant since in recent years there is an increasing interest in utilizing sumac for food and non-food applications due to its unique chemical composition and biological activities, and with its favourable worldwide distribution it appears a widely available renewable feedstock for obtaining alternative phytochemicals using environmentally benign processes, as requested by new worldwide politics for green chemistry, with minimal transportation requirements from source through processing to end consumer [Rayne and Mazza, 2007]. Sumac contains a variety of beneficial compounds, including proteins, minerals, vitamins, unsaturated fatty acids, dietary fibers, and a range of polyphenols (phenolic acids, flavonoids, anthocyanins). Some of the species of the family has shown interesting bioactivity and they have already been used for centuries for food-production and medical purposes. *R. glabra L.* is traditionally used by native Indians of North America in the treatments of bacterial diseases, such as syphilis, gonorrhea, dysentery, and gangrene. The fruits of *R. coriaria* (Sicilian sumac) are commonly used as a condiment in the Mediterranean region and Middle East or as herbal remedy due to its analgesic, antidiarrhetic, antiseptic, anorexic and antihypergylcaemic properties. The extract of *R. coriaria*, which protects humans against oxidative DNA-damage is notable for its

antimicrobial and antioxidant activities. In North America, *R. typhina L.* (staghorn sumac) is used with the pharmacological functions of antihaemorrhoidal, antiseptic, diuretic, stomachic and tonic. In food and beverage formulations the fruit powder has been used as a culinary spice for flavouring and colouring or preservation, for example to inhibit the growth of *Escherichia coli* in ground beef while the fruit extract has been incorporated into wheat bread to extend the mold-free shelf life [Kossah et al., 2011, Mohammadi et al., 2016]. Geographic origins, harvesting seasons, postharvest handling, plant parts, and analytical methods affect the proximate composition of sumac. For the moment, the information on the chemical composition in terms of the types and concentrations of different parts of the plant is very poor, as much as the knowledge about its bioactivity and the molecular mechanisms for these bioactivities. Researchers so far focussed mainly on the two main species *R. coriaria* and *R. thypina*. All of the studies have used either ethanol or water-based extracts. It has been discovered that the wood of staghorn sumac for example, shows antioxidant and antitumorigenic properties. The leaves are proven to be antioxidative. The fruits have been tested antioxidative, anthelmintic, anti-proliferative, anti-inflammatory and antimicrobial showing the greatest effectiveness against Gram-positive bacteria, with Gram-negative strains being more resistant. Nevertheless, not each of these characteristics are generalizable across the *Rhus* genus and further surveys are needed on which are the optimum extraction (e.g., solvent type) and storage conditions for obtaining the highest quality yields of desired functionality. Correct characterization of bioactive phytochemicals in sumac would explain its potential uses for health, nutrition and pharmacology.

CHAPTER 2

Experimental

2.1 Materials

Fresh leaves of sumac were supplied by Snaga Ljubljana and air dried at room temperature before being smashed for the extract preparation. Alkaline-scoured, bleached and mercerized 100% cotton plain-weave fabric, with mass area of 120 g/m^2, wrap density of 51.3 threads/cm and weft density of 30.7 threads/cm was purchased from Tekstina d.o.o. (Ajdovščina, Slovenia). To be able to increase silver adsorption on cellulose fibres, iSys MTX (CHT, Germany) a reactive organic-inorganic sol-gel precursor was applied on cotton fibres. As a precursor of silver nanoparticles, silver nitrate ($AgNO_3$) (purity 99.98%) was used, obtained from Sigma Aldrich. Double-distilled water was used in all experiments.

2.2 Preparation of sumac leaves extract

Dried sumac leaves were finely smashed by hand and poured in double distilled water. The concentration of sumac leaves was 20 g/L. The infusion was kept on fire 20 min, slightly boiling, then cooled down at room temperature. The leaves were separated from the extract through a sieve and the obtained liquid was stored at 2.5°C for further use.

2.3 *In situ* synthesis of AgNPs on cotton fabric

A reactive organic-inorganic sol-gel precursor iSys MTX was hydrolysed in water in a concentration of 15 g/L and applied to the cotton fabric samples using a pad-dry-cure procedure. Firstly, the samples were full immersed in the matrix solution and squeezed on a foulard (Mathis, Switzerland) using a wet pick up of 80±2%. Afterwards, cotton fabric samples were dried at 100°C for 1 min, subsequently cured at 150°C for 4 min to start the condensation reaction between the polysiloxane matrix and the cellulose fibres. To allow a complete silica network formation, the samples were stored for a week under standard atmospheric conditions (65±2% relative humidity and 20±1°C).
In the experiment, five concentrations of $AgNO_3$ water solution were prepared, i.e.: 0.1 mM, 0.5 mM, 1.0 mM, 2.5 mM, 5.0 mM. The *in situ* synthesis of AgNPs on studied cotton fabric samples was performed by a two-step procedure, using the Gyrowash machine (James Heal, Great Britain). In the first step, cotton samples were cut to a dimension of approximately 20 cm × 15 cm to give a mass of 3 g and immersed in 75 mL of different concentrations of $AgNO_3$ water solutions to give a fabric-to-liquor ratio of 1:25 and furtherly stirred in the Gyrowash for 10 min at 60°C. This allowed the Ag^+ ions to be adsorbed and well dispersed all over the fabric. In the second step, 75 mL of the sumac extract

was added reaching the final fabric-to-liquor ratio 1:50. Again, the samples were treated in Gyrowash for another 1 h at 60°C. Afterwards, all the samples were rinsed in distilled water and dried at room temperature. The changed colour of the samples indicated the successful deposition of AgNPs on the fibres. For each studied $AgNO_3$ concentration, ten samples were prepared. Additionally, for the purpose of comparison cotton samples were treated in sumac extract only, whereas instead of $AgNO_3$ solution the aliquot of distilled water was used. The samples' codes are presented in Table 2.1.

SAMPLE CODE	Description of chemical modification
CO_UN	Untreated cotton
CO_M/Oc	Cotton impregnated with matrix and sumac extract
CO_M/Oc+0.1Ag	Ag loaded cotton fabric obtained from 0.1 mM $AgNO_3$ solution
CO_M/Oc+0.5Ag	Ag loaded cotton fabric obtained from 0.5 mM $AgNO_3$ solution
CO_M/Oc+1.0Ag	Ag loaded cotton fabric obtained from 1.0 mM $AgNO_3$ solution
CO_M/Oc+2.5Ag	Ag loaded cotton fabric obtained from 2.5 mM $AgNO_3$ solution
CO_M/Oc+5.0Ag	Ag loaded cotton fabric obtained from 5.0 mM $AgNO_3$ solution

Table 2.1: Sample codes and their description according to the chemical modification used

2.4 Washing fastness

In order to verify the washing properties of the functionalized cotton samples, part of the studied samples were subjected to one or five washing cycles (code 1 W or 5 W) according to the ISO 105-C06 standard method using a Gyrowash (James Heal, Great Britain). Cotton samples were cut in dimension of 10 cm × 4 cm and immersed in 150 mL of SDC (standard detergent solution) of a concentration of 4 g/L with the addition of 10 steel balls. Each washing cycle was performed at 40°C for 45 min. After washing the samples were rinsed twice in distilled water and dried at room temperature.

2.5 Cotton fabric characterization

2.5.1 Scanning electron microscopy (SEM) and energy-dispersive X-ray spectroscopy (EDS)

Morphological changes occurring after the functionalization of cotton samples were studied using a JEOL 6060 LV scanning microscope, operating at 10 kV. Before SEM images were taken, the samples were coated with a thin layer of mixture of platinum and gold to ensure sufficient electrical conductivity and to avoid charging effects. In addition, SEM images of studied cotton samples were taken using a field emission scanning electron microscope, FEG-SEM ThermoFischer Scientific Quattro S (ThermoFischer Scientific, USA) working at an acceleration voltage of 1 kV in high vacuum using a Concentric Backscattered Electron Detector (CBS). To be able to verify the chemical composition of the observed particles, an Oxford Instruments Ultim Max 65 Energy-dispersive Detector (EDS) using an AZtec software was exploited. The functionalized samples were analysed in high vacuum and the acceleration voltage used was 10 kV. This enabled acquisition of the EDS spectrum and element mapping images of C, Ag and O. Before analysis the samples were coated by a thin layer of carbon.

2.5.2 Inductively coupled plasma mass spectroscopy (ICP-MS)

The concentration of Ag in the studied functionalized cotton samples was determined by ICP-MS using a Perkin Elmer SCIED Elan DRC spectrophotometer. Prior to measurements, each of the studied

fabric sample with a mass of 0.5 g was decompose in acid consisting of 65% nitric acid (HNO_3) and 30% hydrogen peroxide (H_2O_2) using a Milestone microwave system. Two measurements were taken for each sample, and the Ag concentrations are reported as mean values.

2.5.3 UV protection properties

In order to verify UV protection of the functionalized cotton samples before and after repetitive washings, each sample was analysed using a Varian Cary 1E UV/Vis spectrophotometer (Varian, Australia), containing a DRA-CA-301 integration sphere and Solar Screen software. The transmission was evaluated in a wavelength range 280–400 nm. Each sample was scanned six times at different angles of orientation of the warp. In this manner the averaged transmission (T) of the ultraviolet radiation through the studied samples were obtained, i.e. at the wavelengths between 315 and 400 nm (UV-A), 280 and 315 nm (UV-B) and 280 and 400 nm (UV-R). The ultraviolet protection factor (UPF) was calculated using the following equation (2.1) [Lee, 2009]:

$$UPF = \frac{\sum_{\lambda=280}^{400} E_\lambda S_\lambda \Delta\lambda}{\sum_{\lambda=280}^{400} E_\lambda S_\lambda T_\lambda \Delta\lambda} \tag{2.1}$$

where E_λ is the relative erythemal spectral effectiveness, S_λ is the solar spectral irradiance, T_λ is the spectral transmittance of the specimen, and $\Delta\lambda$ is the measured wavelength interval in nm. The UPF rating and UVR protection categories were determined from the calculated UPF values, according to the Australian/New Zealand Standard: Sun protective clothing – Evaluation and classification [AS/NZS, 2017] and are presented in Table 2.2.

UPF Rating	Classification	Shere of UV radiation blocked (%)
15	minimum	93.3
30	good	96.7
50, 50+	excellent	98.0

Table 2.2: Ultraviolet protective factor (UPF) classifications according to the Australian/New Zealand Standard: Sun protective clothing – Evaluation and classification

2.5.4 Colour measurements

The colour measurements of the studied functionalized cotton samples before and after washing were evaluated using a Datacolor Spectraflesh 600 PLUS-CT spectrophotometer. The mesurements were performed with a 9 mm aperture under D65 illumination and an observation angle of 10°. For each studied sample the average of then mesurements of CIELAB color coordinates was provided, and the color difference, ΔE^*, was calculated using the Equation 2.2 [Berger-Schunn, 1994].

$$\Delta E^*{}_{ab} = \sqrt{(\Delta L^*)^2 + (\Delta a^*)^2 + (\Delta b^*)^2} \tag{2.2}$$

where ΔL^*, Δa^* and Δb^* are differences between the color coordinates between the unwashed and washed samples.

2.5.5 Antibacterial activity

Antibacterial activity of the AgNPs loaded samples was tested for both Gram-positive *Staphylococcus aureus* (*S. aureus*, ATCC 6538) and Gram-negative *Escherichia coli* (*E. coli*, ATCC 25922) bacteria according to the standard method AATCC 100. The procedure included following steps: preparation of the samples and agar plates, preparation of the bacteria inoculum, inoculation of the samples, bacteria colony counting and evaluation of antibacterial activity.

Preparation of agar plates and the samples

For the preparation of agar plates, LB (Luria broth, Sigma-Aldrich) broth of 25 g/L was mixed with distilled water. Subsequently agar powder (Sigma-Aldrich) was added to the mixture at the concentration of 15 g/L. The flasks were treated in autoclave for 30 min at 120°C. Afterwards, the solution was cooled down to approximately 60°C and aseptically poured in plates by a thin layer, just to cover the bottom of the plates. The plates were left to solidify and stored in the fridge for further use. The studied samples were cut in a pieces of 3 cm × 3 cm in dimension, placed in a 50 mL flask and closed with cotton wadding and aluminium foil. For each studied samples three parallels of test swatches were prepared. The capped flasks containing untreated control and functionalized test swatches were than sterilized in autoclave for 30 min at 120°C.

Preparation of bacteria inoculum

The chosen bacteria, *S. aureus* or *E. coli*, was taken by the stock frozen at -80°C. With a sterilized needle, a small portion of bacteria stock was diluted in 10 mL of nutrient LB medium and incubated by a constant shaking at 200 rpm at 37°C for 24. Overnight bacteria inoculum was furtherly refreshed to eliminate death bacteria cells. For this purpose 0.2 mL of overnight bacteria inoculum was diluted by a 10 mL of LB medium and left in an incubator until reaching the optical density (OD) between 0.4 and 0.6, denoting the exponential growth of bacteria in the inoculum. The latter was determined by UV-VIS analysis at wavelength of 475 nm. Once reached an optimum OD, the bacterial inoculum was diluted by a LB media using a 1500 µL safety cap until reaching the OD of 0.28, meaning the bacteria concentration of 2.8×10^8 bacteria/mL .

Inoculation of the samples

Using LB media, the bacteria inoculum was furtherly diluted up to 10^{-3} in order to reach prescribed bacteria concentration of $1–3 \times 10^5$. Afterwards, 500 µL of prepared bacteria inoculum was ascetically poured in each flask containing untreated control and functionalized test swatches, closed tightly with cotton wadding and aluminium foil and incubated for 24 h at 37°C. After the incubation, 20 mL of highly purified sterilized water (MQ) was poured into each flask.

Bacteria colony counting

After adding 1350 µL MQ water, each flask was vigorously shaken for 1 min. The resulting bacteria dispersion was furtherly appropriately diluted (up to 10^{-4}). Aliquot of 40 µL was aseptically spread over agar plates using a glass triangle stick. Four to five agar plates were inoculated for each parallel of control untreated and functionalized tested swatches. The inoculated agar plates were than incubated at 37°C for 24 h. After incubation bacteria colonies forming units (CFU) grown overnight were counted.

Evaluation of antibacterial activity

The percent reduction of bacteria (R) due to the presence of silver nanoparticles was evaluated according to the following formula (2.3) [ASTM, 2001]:

$$R = \frac{B - A}{B} 100[\%] \tag{2.3}$$

where B is the averaged number of CFU recovered from the inoculated untreated control specimen swatches in the jar incubated over 24 h, and A is the number of bacteria recovered from the inoculated functionalized test specimen swatches in the jar incubated over 24 h.

CHAPTER 3

Results and Discussion

3.1 Surface morphology

Surface morphology and quality of Ag NPs deposition on fabric were evaluated with scanning electron microscopy (Figure 3.1). The SEM photomicrographs revealed that the treatment with silica matrix did not altered the morphology of the fabric, which appeared with uniform neat plain spun structures as the control cotton fabric.

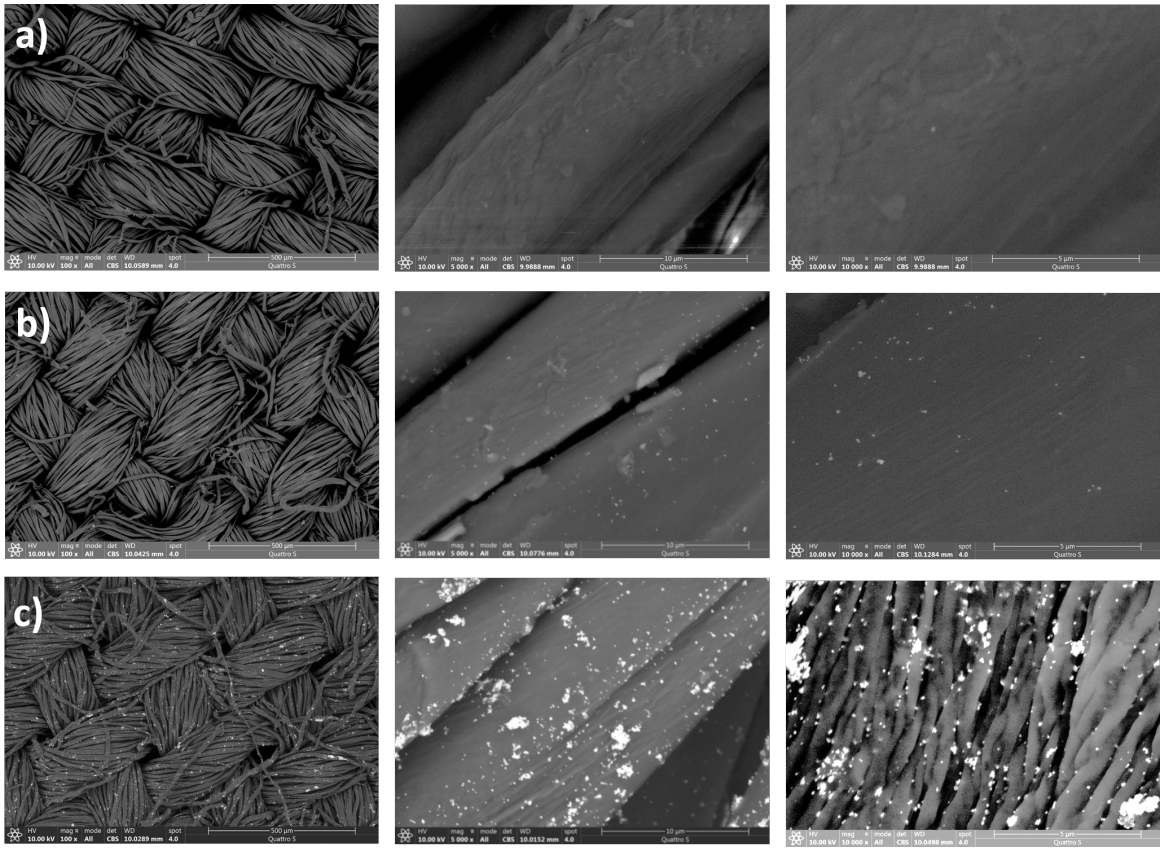

Figure 3.1: SEM images at different magnification, from left to right: 100x, 5kx, 10kx. Samples: a) sample CO_M/Oc+0.1Ag, b) sampleCO_M/Oc+1.0Ag, c) sample CO_M/Oc+5.0Ag.

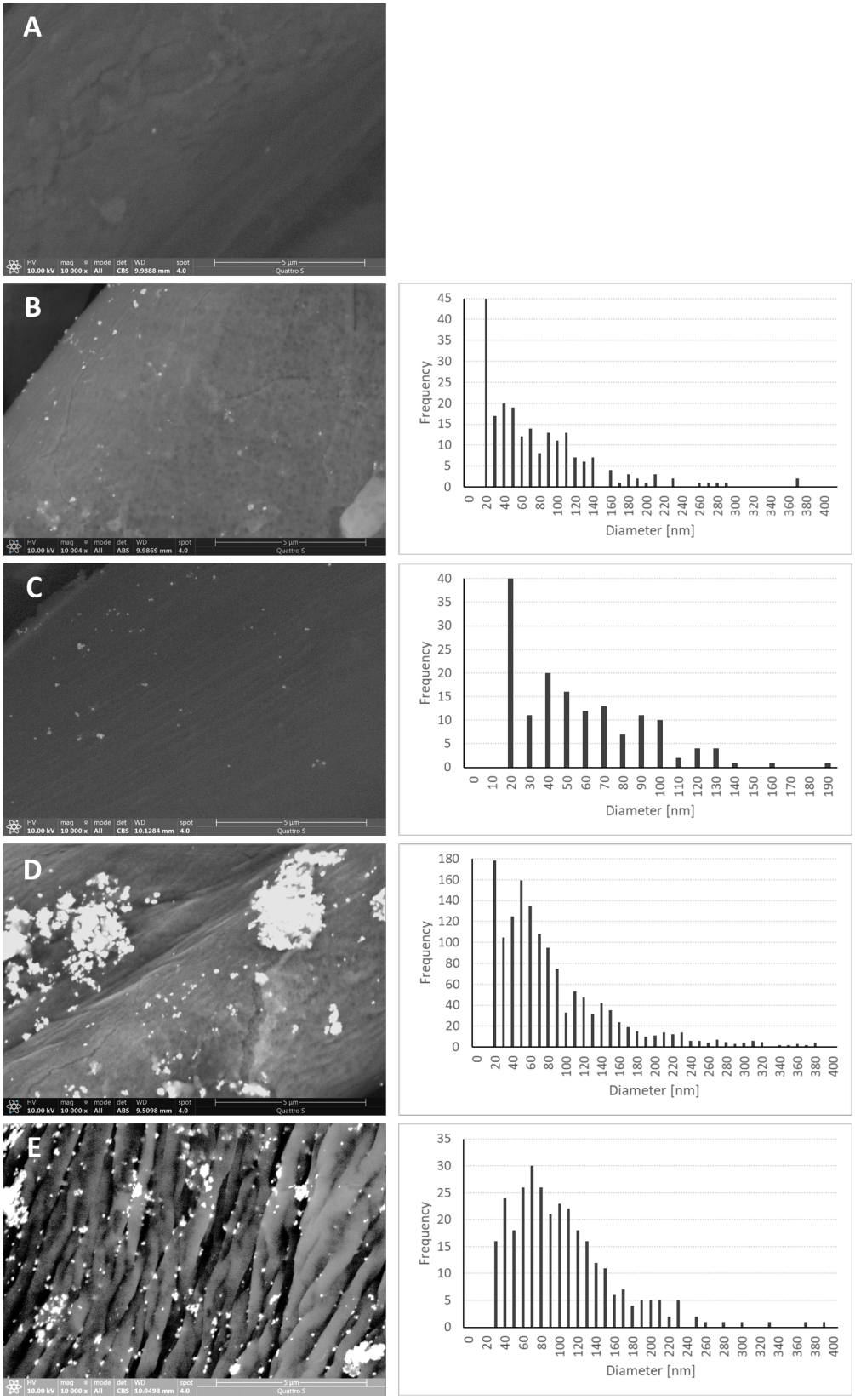

Figure 3.2: SEM-BSE images of cotton fibres with Ag NPs reduced with sumac at magnification 10000x and particle size distribution: A) sample CO_M/Oc+0.1Ag, B) sample CO_M/Oc+0.5Ag, C) sample CO_M/Oc+1.0Ag, D) sample CO_M/Oc+2.5Ag, E) sample CO_M/Oc+5.0Ag.

The surface of the fibres showed debris and ripples on it, due to the nature of the cellulose fibres themselves. All the silver-treated samples were evaluated as well, nevertheless, even at the highest magnification the presence of Ag NPs could not be detected, as it was impossible to distinguish them from the roughness of cellulose fibres and possible sumac leaves debris. This led to perform SEM micrographs using back scattered electron (BSE) imaging in order to emphasize and expose the difference between the applied particles and the cotton fibre-matrix.

From photomicrographs of the studied samples taken at lower magnification it is possible to see the obvious increase of the Ag NPs content between the samples treated in solutions with increasing $AgNO_3$ concentration. Accordingly, on the surface of the CO_M/Oc+0.1Ag sample only a few NPs were detected, due to the low concentration of $AgNO_3$ (0.1 mM) during the synthesis process. The Ag NPs appeared small, very well dispersed and no aggregations were found among the fibres. By increasing the concentration of $AgNO_3$ (1.0 mM) during the synthesis process, more particles were formed on the surface of the fibres and the number of aggregates increased as well, nevertheless, an even distribution of Ag NPs all over the fibres surface was observed for the sample CO_M/Oc + 1.0Ag. The sample treated with 5.0 mM $AgNO_3$ showed greater amount of Ag NPs on the surface of the fibres, and inside the twisting as well. Was also possible to notice an uneven distribution in size due to the agglomeration, caused by higher concentration of Ag NPs synthetized at this $AgNO_3$ concentration.

Average particle size and particle size distribution were analysed through the ImageJ software using SEM-BSE images taken at higher magnification (10 kx). The values presented gather an average of more measurement of particles obtained from different images. In the case of CO_M/Oc + 0.1Ag sample the extremely low content of Ag NPs was detected, making the particle size analysis impossible to perform, due to the poor data collection. For other studied samples the size distributions are reported in Figure 3.2. The collected results suggested that the variation of the $AgNO_3$ concentration brought to different size of Ag NPs starting from 70 nm for sample synthetized with 0.5 mM $AgNO_3$, 90 nm for the sample treated with 2.5 mM $AgNO_3$ and 100 nm for the highest concentration of $AgNO_3$, 5.0 mM. The higher is the amount of Ag NPs, the higher is the dimension of particles, most likely due to the agglomeration process that occurred during the nucleation and deposition of the NPs. Moreover, also the particle size distribution results were influenced by $AgNO_3$ concentration, not only because shifted towards bigger size but also because the distribution appeared slightly wider in size and less uniform when agglomeration occurred, while it resulted smaller and more homogeneous when the Ag NPs content was reduced.

Energy-dispersive spectroscopy (EDS) was used to prove the effective presence of Ag NPs on the fibre surface. The elemental profile was performed on each sample of silver-treated fabric. A characteristic peak at 3 k due to silver appeared in spectra of all studied samples, confirming the formation of Ag NPs on the fibres surface. In Figure 3.3 only the spectrum of the sample CO_M/Oc+5.0Ag is shown, due to the presence of big agglomerates, which facilitated the EDS analysis of the particles by avoiding the interference of the fibres. In this case silver was the predominant element detected. In addition, element mapping images of C, Ag and O were also performed in this sample in order to verify the homogeneity of the Ag NPs distribution. The results shown in Figure 3.4 suggested a good dispersity of the Ag element on fibres surface, along with intrinsic elements of cotton cellulose fibres, C and O. The ICP MS analysis was performed on all the Ag NPs loaded samples, unwashed and washed one and five times, to quantify the effective concentration of silver deposited on cotton fibres. Results are exposed in Figure 3.5. As expected from previous morphological analysis, an increase in the concentration of $AgNO_3$ in the synthesis process led to a higher content of silver found on the textile. Repetitive laundering caused the leaching of the NPs from the fibres, especially where the content of metal was the highest. The data can be explained considering that the higher was the amount of NPs attached to the surface, the lower was the adhesion to the silica matrix, and higher was the possibility for formed aggregates to be washed away. In this regard, is possible to highlight

that the sample synthesised with 0.1 mM and 0.5 mM of $AgNO_3$ showed the best washing resistant with low variation in concentration, also after five washing cycles.

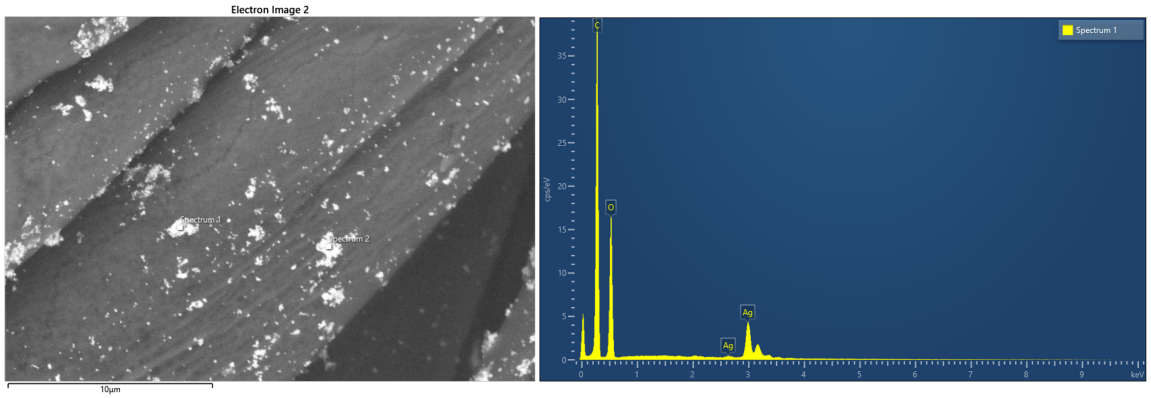

Figure 3.3: EDS spectrum acquired from Ag loaded cotton fabric sample CO_M/Oc+0.5Ag.

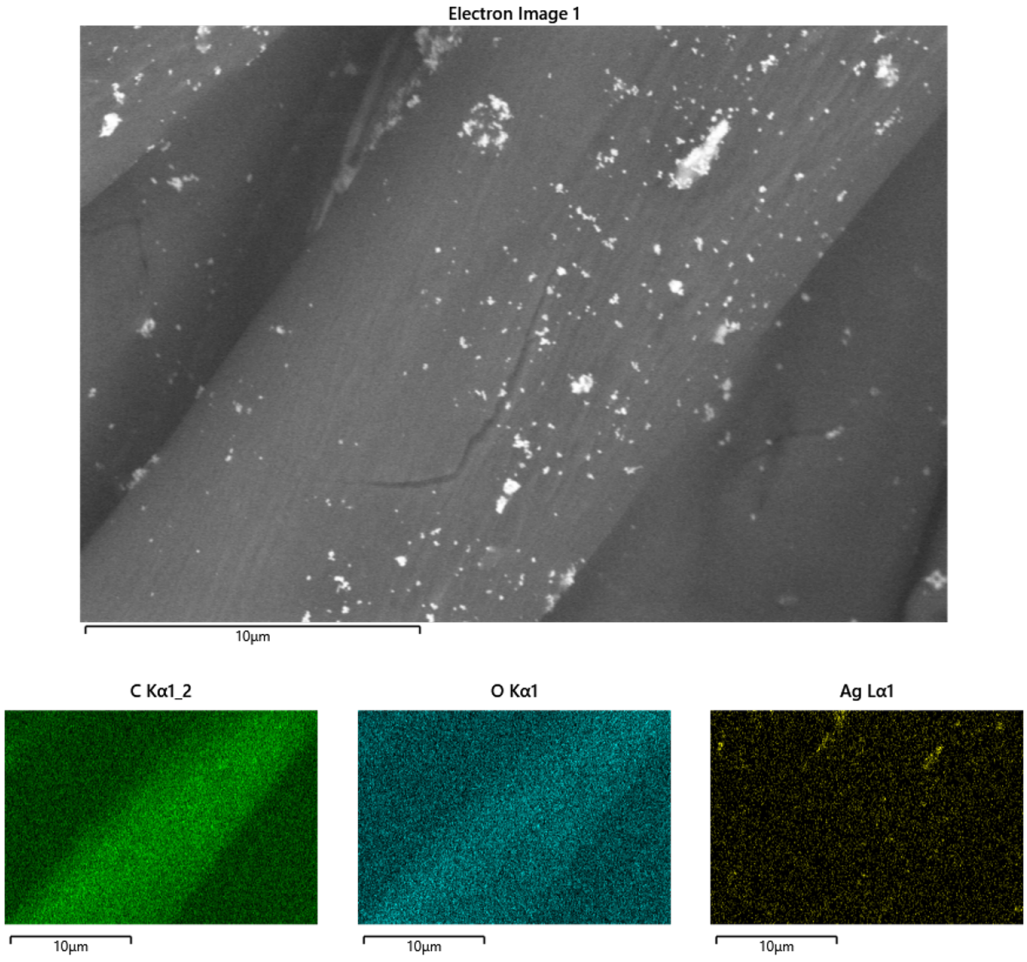

Figure 3.4: Element mapping images of C, O and Ag on the CO_M/Oc+0.5Ag sample.

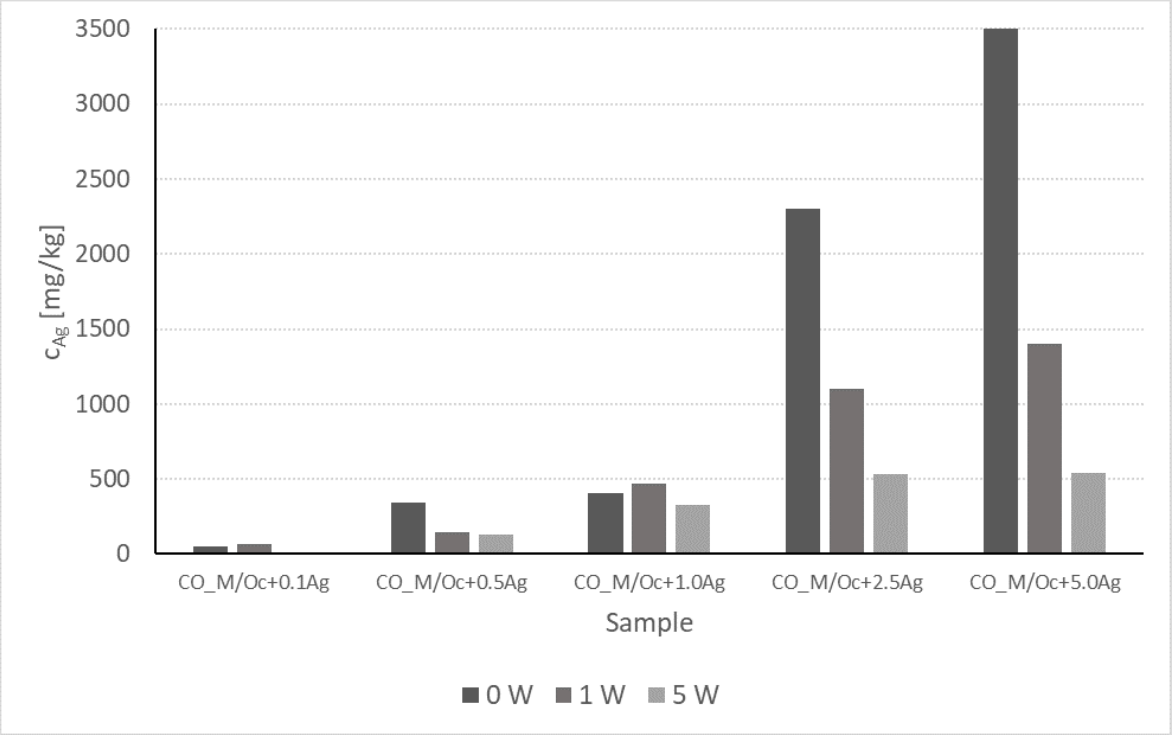

Figure 3.5: Silver concentration C_{Ag} [mg/kg] of the studied samples before (0 W) and after one (1 W) and five (5 W) consecutive washings.

3.2 Colour assessment

The functionalization of cotton fabric with a combination of sumac extract and $AgNO_3$ solution lead to a strong impact on dyeability: significant colour changes occur due to both, treatment with sumac extract and deposition of Ag NPs on the fibres. These colour changes were quantitatively evaluated by the CIE L^*, a^*, b^* coordinates and determination of the colour difference (ΔE^*) between the unwashed and washed samples, which enabled colour fastness assessment. The results are presented in Figure 3.6 and 3.7 and Table 3.1. Values of lightness (L^*) were higher, corresponding to lighter shades, for cotton sample treated with sumac extract only, which as a natural dye conferred a yellowish colour to the fabric (Figure 3.6 and Table 3.1). Successful formation of Ag NPs on cotton fibres was additionally confirmed by a colour change of the studied samples. As observed from Figure 3.6 and Table 3.1 the colour of the Ag NPs loaded cotton fabric changed from yellowish green to fade brownish red and further to fade bluish-red as the concentration of Ag NPs increased. This change of the colour of the studied samples reflected in a slight decrease of the L^* value, while values of green-red coordinate a^* firstly increased by increasing the concentration of Ag NPs on cotton fibres, while again decreased as the concentration of $AgNO_3$ in the synthesis bath increased above 2.5 mM. On the other hand, by increasing the concentration of the Ag NPs on the studied cotton samples, the values of the coordinate b^* decreased from yellow to blue shades, but did not reach the negative values, even at the highest studied concentration of $AgNO_3$ in the synthesis bath. Repetitive washings resulted in lightening of the samples colour, which can be clearly seen in Figure 3.6 and further supported by a gradual increase of the L^* values after one and five washings of the samples. In addition, after washing the Ag NPs loaded samples turned to be slightly more blueish as the values of the b^* coordinate gradually decreased. Intensity of desorption of the sumac extract after multiple washings was further studied by determination of ΔE^* (Figure 3.7) between washed and

unwashed samples. For most of the samples ΔE^* values higher than 5 were obtained, confirming rather poor colour fastness of the samples. However, in respect to the sample CO_M/OC, the presence of Ag NPs at lower concentration (i.e. samples CO_M/OC+0.1Ag; CO_M/Oc+0.5Ag and CO_M/Oc+1.0Ag) improved colour fastness. Contrary, ΔE^* of the samples with higher Ag content (i.e. samples CO_M/Oc+2.5Ag and CO_M/Oc+5.0Ag) strongly increased, which could be explained by the increase in leaching of Ag NPs during washing cycles and a corresponding higher loss in colour intensity. Namely, from the SEM-BSE images higher agglomerates were detected in the case of these two samples, meaning that they could be more easily removed from the fibres surface as did smaller particles in the case of samples treated with lower concentration of $AgNO_3$.

SAMPLE CODE	Washings	L^*	a^*	b^*
CO_M/Oc	0 W	85.7	-2.63	20.35
	1 W	87.27	0.07	13.89
	5 W	86.41	0.34	10.59
CO_M/Oc+0.1Ag	0 W	86.73	-2.24	19.97
	1 W	83.24	1.29	16.93
	5 W	84.8	0.16	11.76
CO_M/Oc+0.5Ag	0 W	80.39	-0.63	18.45
	1 W	80.43	2.05	15.08
	5 W	80.4	1.68	14.05
CO_M/Oc+1.0Ag	0 W	69.25	2.28	15.53
	1 W	73.26	2.74	14.15
	5 W	75.66	2.23	11.42
CO_M/Oc+2.5Ag	0 W	60.87	1.41	12.39
	1 W	67.48	1.47	9.84
	5 W	70.28	1.1	8.7
CO_M/Oc+5.0Ag	0 W	55.78	0.91	11.66
	1 W	65.38	1.18	9.57
	5 W	69.23	1.21	9.25

Table 3.1: CIE L^*, a^* and b^* coordinates of the studied samples before (0 W) and after one (1 W) and five (5 W) consecutive washings.

Figure 3.6: Photo images of the studied samples before (0W) and after one (1W) and five (5W) consecutive washings.

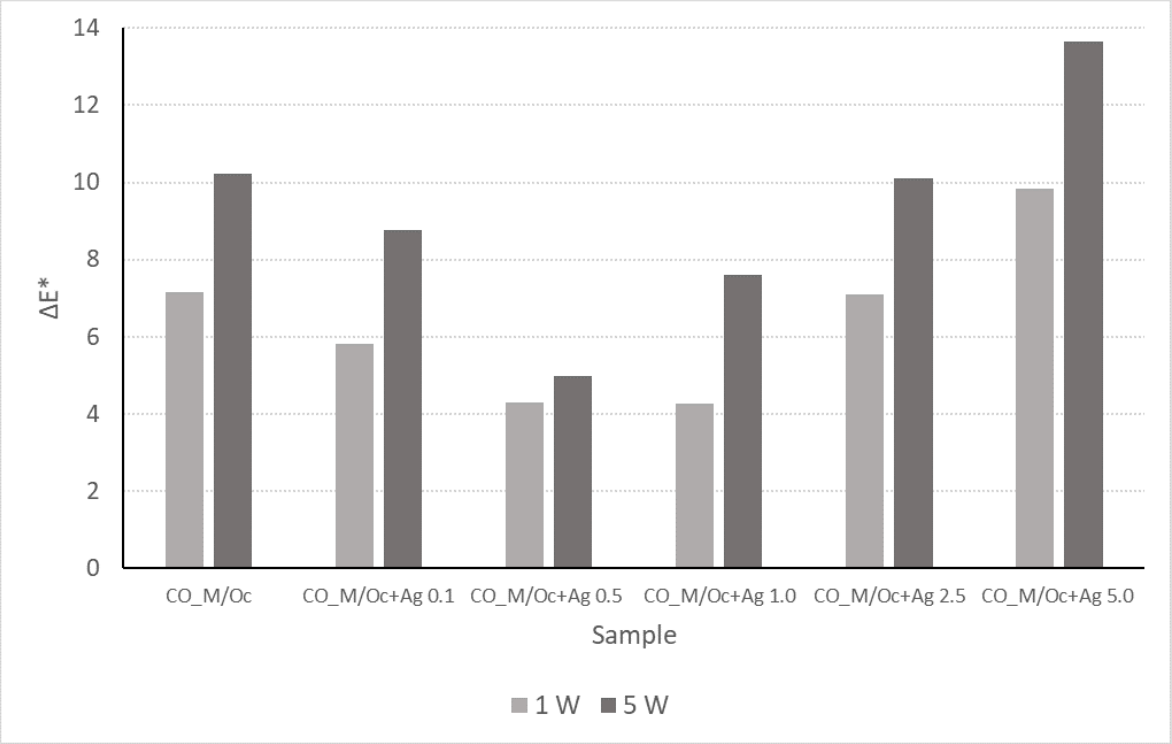

Figure 3.7: Colour difference, ΔE^*, of the studied samples, determined between unwashed and washed once (1 W) and five (5 W) times.

3.3 Bacterial reduction

Antibacterial activity of Ag NPs treated cotton samples, before and after washing, was evaluated against Gram-negative bacterium *E. coli* and Gram-positive bacterium *S. aureus*, using colony counting method. The respective values of microbial reduction are shown in Figure 3.8 - 3.10. Cotton sample did not reflect any antimicrobial activity confirming to be a suitable substrate for bacterial growth, well seen from the photography of petri-dishes in Figure 3.8. The sumac leaves extract alone (sample CO_M/Oc) revealed excellent antibacterial activity against *S. aureus* (R> 97%), but did not reduce the growth of *E. coli*, showing to be perfect breeding ground for the growth of the studied Gram-negative bacteria, resulting in negative values of R (R<-20%) (Figure 3.9). This means that the presence of sumac extract even promoted the growth of *E. coli* on cotton fabric. This results are in accordance with the literature [Nasar-Abbas and Halkman, 2004, Rayne and Mazza, 2007, Wang and Zhu, 2017], where it was found out that phenolic compounds of the sumac extract either in water or alcohol are strong antibacterial agents only against Gram-positive bacteria, while their antimicrobial activity against Gram-negative bacteria are rather poor. In this context, the antibacterial contribution of Ag NPs appeared to act synergistically with the sumac extract, as excellent reduction of *S. aureus* growth (R>98%) was obtained in the presence of all samples functionalized with Ag NPs independently from the concentration of $AgNO_3$ used in the synthesis bath. Contrary, to obtain sufficient protection against *E. coli* higher concentration of $AgNO_3$ and thus Ag NPs was needed. It can be seen from the results in Figure 3.9 that the treatment of the cotton with the smallest studied concentration of $AgNO_3$ (sample CO_M/Oc+0.1 Ag) could only slightly overcome the good growth conditions provided by the presence of the sumac extract.

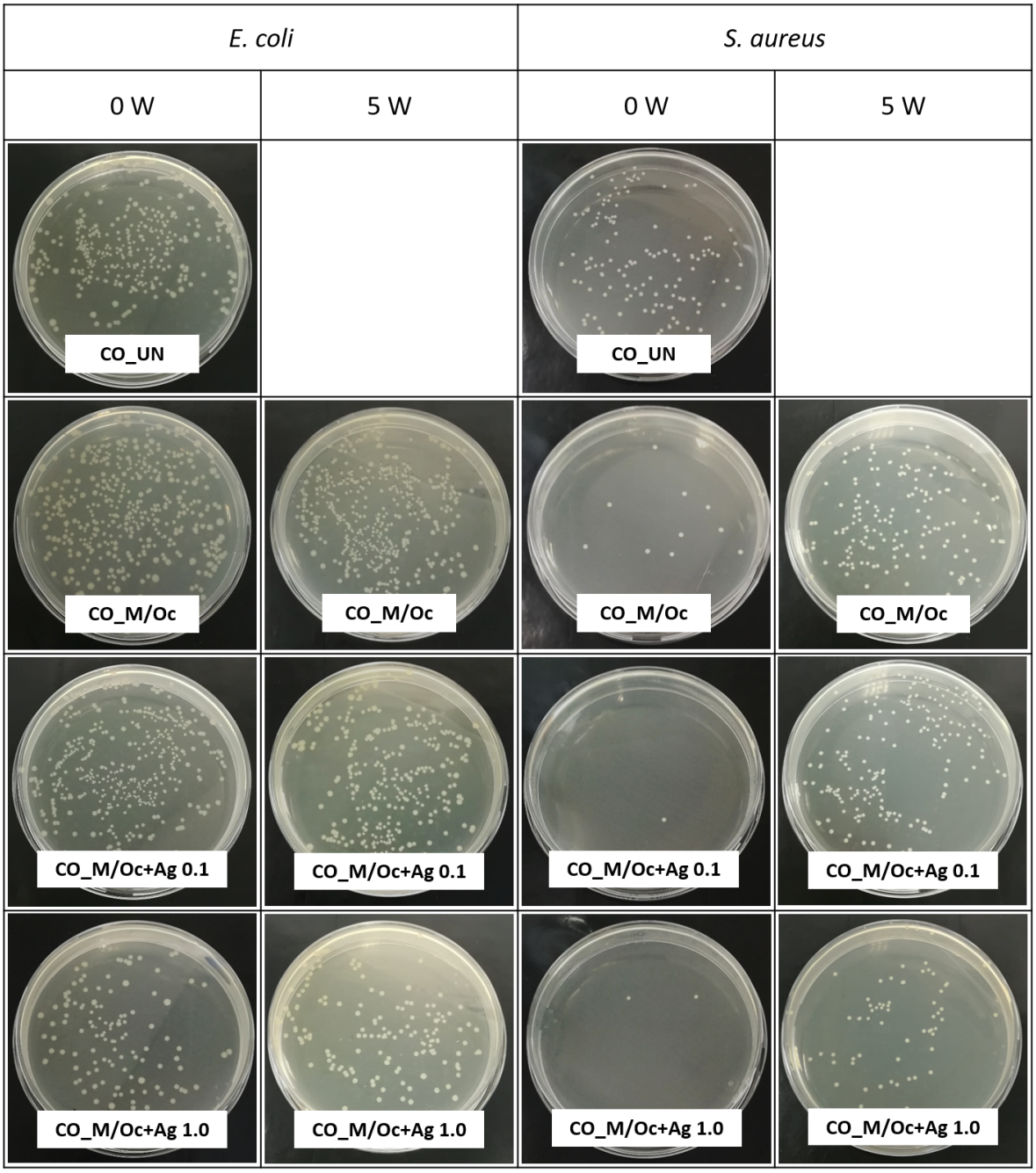

Figure 3.8: Photographs of antibacterial activity against *E. coli* (right side) and *S. aureus* (left side) of the cotton fabrics untreated, treated with sumac extract and treated with different concentrations of $AgNO_3$.

Accordingly, a value of R close to 0% was achieved for the CO_M/Oc+0.1Ag. However, slight increase of the silver content on cotton sample CO_M/Oc+0.5Ag already resulted to be enough to establish excellent antimicrobial activity (R>98%). The plant compounds were desorbed from the cotton fibres during the washing of the sample CO_M/Oc, showing poor washing durability.

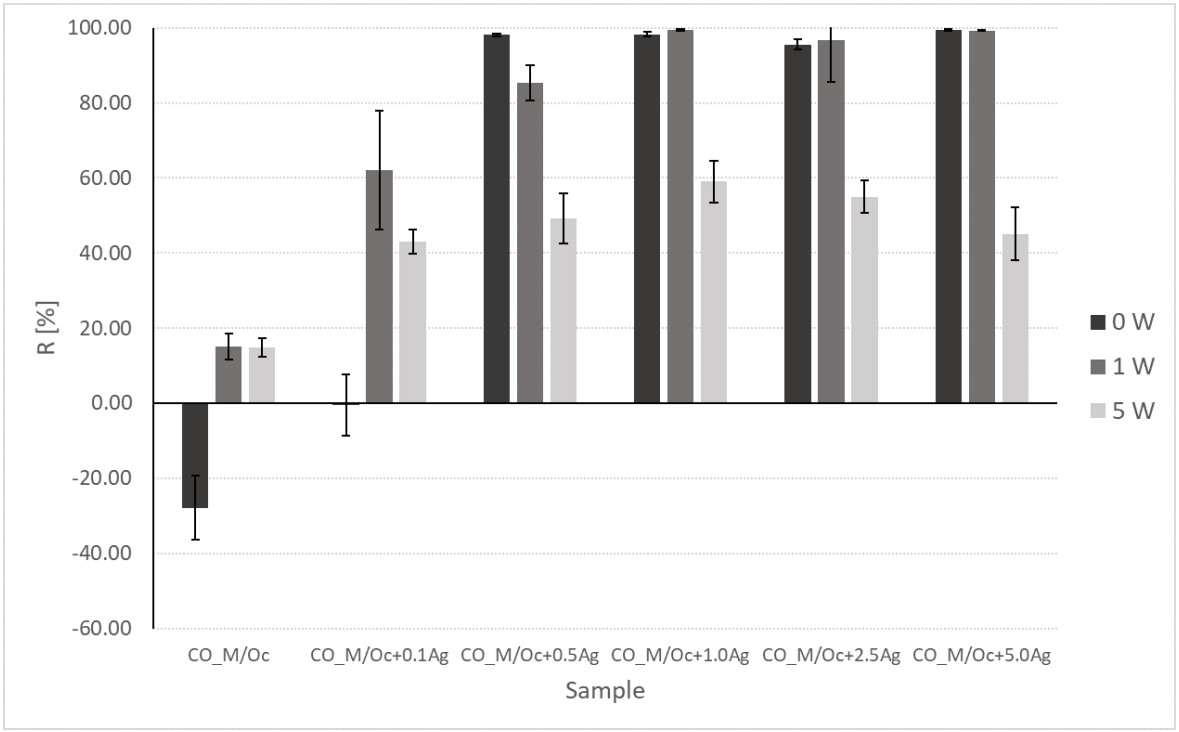

Figure 3.9: Bacterial reduction R of *E. coli* determined for the studied samples before (0 W) and after one (1 W) and five (5 W) consecutive washings.

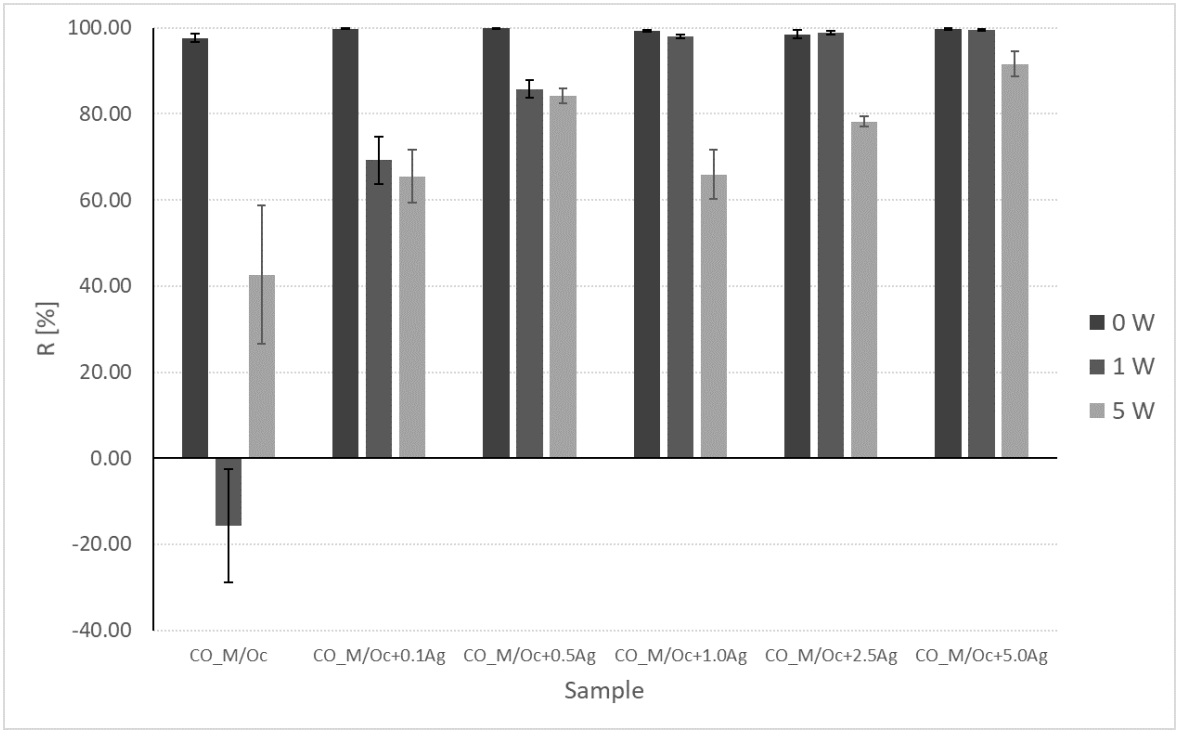

Figure 3.10: Bacterial reduction R of *S.aureus* determined for the studied samples before (0 W) and after one (1 W) and five (5 W) consecutive washings.

Washing the samples reflected in a strong decrease of the antibacterial activity against *S. aureus*, while growth of *E. coli* was comparable to that obtained for the untreated cotton. Washing durability of Ag NPs, on the other hand, was clearly concentration dependent. The higher the initial concentration of the Ag NPs, the higher was the retained antimicrobial activity after washing. Accordingly, after first washing sufficient reduction growth of *S. aureus* and *E. coli* with a value of R>60% was obtained in the case of CO_M/Oc+ 0.1Ag sample, while biocidal activity with growth reduction of R>96% was provided only by treatment with ten times higher $AgNO_3$ concentration, i.e. sample O_M/Oc+1.0Ag. Five consecutive washings of the studied samples resulted in a complete loss of a sufficient protection against *E. coli*, while excellent antibacterial activity against *S. aureus* with a value of R>90% was still preserved for the CO_M/Oc+5.0Ag sample treated with the highest studied concentration of $AgNO_3$ in the synthesis bath. To gain better insight into antibacterial activity of newly synthesized Ag NPs plot Ag concentration of the studied unwashed and washed samples determined by ICP MS versus bacterial reduction was obtained (Figure 3.11). The results confirm the effect of the content of silver on the growth inhibition of bacteria: the higher the concentration, the higher the bactericidal effect. Importantly, it is possible to observe that four times lower concentration of Ag was needed on cotton fibres to obtain moderate 60% growth reduction of *S. aureus* in comparison to *E. coli*. Accordingly, minimal inhibition concentration (MIC) against *S. aureus* was determined at 15 mg/kg of silver, while MIC against *E. coli* was set at 70 mg/kg of Ag. This undoubtedly confirms different antimicrobial action of Ag NPs between Gram-positive and Gram-negative bacteria, whereas higher antibacterial activity of the newly synthesized Ag NPs against *S. aureus* is well seen. This is not in accordance to the results reported by others [Feng et al., 2000, Stular et al., 2017, Patil et al., 2019], demonstrating equal or higher antibacterial activity of Ag NPs against Gram-negative bacteria. Nevertheless, to obtain complete 100% bacterial reduction and thus biocidal activity approximately the same concentration of Ag was needed regardless of the bacteria type. Accordingly, the minimal biocidal concentration (MBC) was determined at 340 mg/kg of silver for *S. aureus* and *E. coli*. The reason for such behaviour is hard to explain, since mechanism of bactericidal action of Ag NPs is still not well understood. However, in general different antibacterial activity of Ag NPs between both types of bacteria is ascribed to structural and compositional differences of bacterial cells. Antimicrobial activity of silver-based materials has been described according to different mechanisms, as presented in teoretical part.. The main antimicrobial mechanism is ascribed to the ability of released Ag^+ ions in the presence of moisture, which reacts with –SH functional groups of proteins, resulting in their inactivation. Additionally, Ag^+ ions can also penetrate in the bacterial cell wall, reflecting in the impairment of the bacterial cells. In this respect, the presence of peptidoglycans in the bacterial cell wall acts as a protection against Ag in both types of bacteria. Since peptidoglycans exist in higher concentration in the cell wall of Gram-positive bacteria, this was the main reason employed for the observed higher antibacterial activity against Gram-negative *E. coli* in comparison to *S. aureus* in the literature. Additional possible mechanism for the antibacterial activity of Ag NPs can also be explained in terms of generated ROS [Rehan et al., 2019]. ROS are known to be highly reactive ionic species (O^{2-}, HO•, H_2O_2, O_2), which has the ability to damage the bacterial cells trough oxidative stress. As explained in teoretical part, ROS generates as a result of a redox processes during the exposure of semiconductor NPs to UV or visible light [Kumar et al., 2017, Singh et al., 2018]. In this respect, positively charged Ag NPs are well trapped in thicker peptidoglycan layer of Gram-positive bacteria as compared to the thin peptidoglycan layer of Gram-negative bacteria [Tsuneda et al., 2004, Kumar et al., 2017]. Accordingly, trapped Ag NPs must have produced sufficient amount of ROS, resulting in the damage to the bacterial cell, thus reflecting observed higher antibacterial activity against Gram-positive *S. aureus* in comparison to *E. coli*. Therefore, we can assume that the mechanism of antimicrobial activity of newly synthesized Ag NPs was in favour to Ag NPs ability to penetrate inside the bacterial cell and ROS formation, rather than just Ag^+ release. However, to confirm this assumption additional analysis would have to be obtained, which go beyond the purpose of our study.

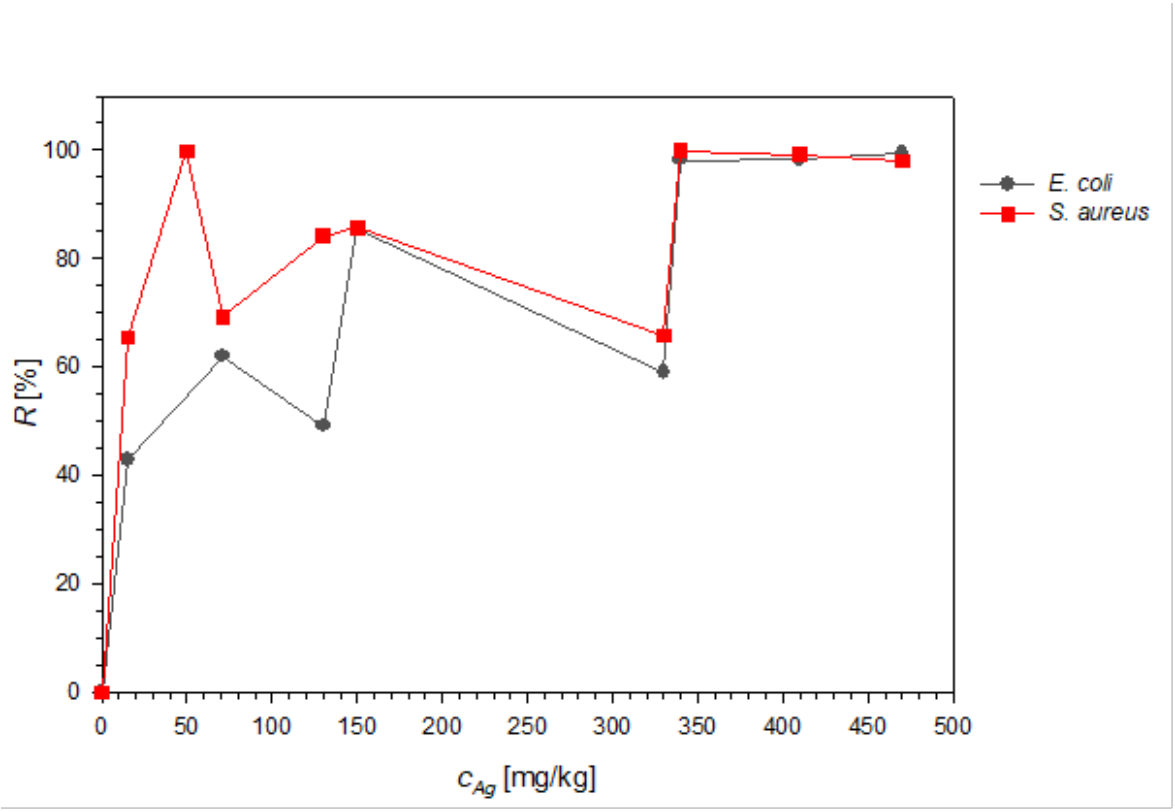

Figure 3.11: Relation between bacteria reduction R [%] with silver concentration C_{Ag} [mg/kg] determine on the studied unwashed and washed samples.

3.4 UV Protection

UV radiation is beneficial to the human body because it sterilizes and promotes vitamin D synthesis in the body. However, high levels of UV radiation could result in sunburn and, penetrating deep into the skin, could cause ultraviolet mutagenesis, that is, damage to skin cells at the gene level; its most terrible complication is melanoma, a tumour of the skin. UV protective textiles can provide effective protection against such damages [Yu et al., 2020]. The wavelength range of solar ultraviolet radiation is located between 200 and 400 nm and can be classified into three distinct regions including solar UVA (from 320 to 400 nm), solar UVB (from 280 to 320 nm), and solar UVC (from 200 to 280 nm). The solar UVC area, the most dangerous to humans, is completely absorbed by the ozone atmospheric cover, thus, the UV shielding of fabrics/fibres is mainly attributed to their resistance to UVA and UVB solar regions. To evaluate UV protection properties of the studied samples UPF was determined from the transmission properties in the UV range according to the equation 2.1 (see page 21 in Experimental part). In addition the transmission (T) and reflection (R) properties of the studied samples were determined in the UV-vis range 200–800 nm. Results of the UPF determination are shown in Figure 3.12 and Table 3.2. In accordance with the AS/NZS test standard, studied samples were additionally classified according to the quality of the UV protection, i.e. as minimum (demonstrating UPF in the range 0–15) , good (demonstrating UPF in the range 16–30) and excellent (UPF above 30) [Ren et al., 2016, Sun and Tang, 2011, Zhou et al., 2014]. As expected, untreated cotton sample demonstrated weak UV-protection ability, as more than 30% of UV rays could be transmitted through the porous structure of the CO_UN sample. Accordingly, an UPF of only 3.8 was determined for CO_UN sample. The presence of silica matrix did not impart any UV protection properties, as

CO_M sample transmitted approximately 20% of UV rays, thus showing an UPF of 5.0. On the other hand, treatment of cotton fabric with the sumac leaf extract resulted in a significant decrease of the UV transmission. Namely, CO_M/Oc sample showed excellent, over 95% blocking ability of the UV radiation, which reflected in the UPF of 51.11. Accordingly, it can be assumed that such excellent UV protection could be attributed to the UV absorbing ability of the aromatic phenolic compounds present in the water extract.

SAMPLE CODE	W[a)]	Mean UPF	T [%]			Blocking [%]		UPF rating	UVR prot. cat.
			UVA	UVB	UVR	UVA	UVB		
CO_UN		3.76	29.34	25.35	28.39	70.66	74.65	4	M
CO_M		5.02	25.03	18.67	23.58	74.97	81.33	5	M
CO_M/Oc	0 W	51.11	3.69	1.73	3.25	96.31	98.27	50	E
	1 W	41.75	6.43	2.12	5.49	93.57	97.88	40	E
	5 W	29.50	8.63	3.05	7.42	91.37	96.95	30	G
CO_/Oc+0.1Ag	0 W	40.50	4.80	2.16	4.22	95.20	97.84	40	E
	1 W	36.75	6.01	2.48	5.24	93.99	97.52	40	E
	5 W	29.53	7.89	3.09	6.85	92.11	96.91	30	G
CO_M/Oc+0.5Ag	0 W	47.91	3.73	1.87	3.32	96.27	98.13	50	E
	1 W	33.59	6.25	2.71	5.47	93.75	97.29	30	G
	5 W	33.24	6.40	2.76	5.61	93.60	97.24	30	G
CO_M/Oc+1.0Ag	0 W	60.87	2.76	1.47	2.47	97.24	98.53	60	E
	1 W	36.71	4.98	2.49	4.44	95.02	97.51	40	E
	5 W	36.25	5.56	2.54	4.90	94.44	97.46	40	E
CO_M/Oc+2.5Ag	0 W	55.67	2.37	1.73	2.15	97.63	98.27	60	E
	1 W	56.24	3.53	1.63	3.11	96.47	98.37	60	E
	5 W	36.92	4.84	2.52	4.33	95.16	97.48	40	E
CO_M/Oc+5.0Ag	0 W	69.07	1.84	1.38	1.69	98.14	98.62	70	E
	1 W	40.18	3.79	2.31	3.46	96.21	97.69	40	E
	5 W	35.18	4.70	2.67	4.25	95.30	97.33	40	E

a) Washings

Table 3.2: Mean ultraviolet protection factor, UPF, UPF rating and UVR protection categories (M- minimum, G- good, E- excellent according to the Australian/New Zealand Standard: Sun protective clothing – Evaluation and classification) for the untreated and differently coated samples, unwashed and washed once (1 W) and five times (5 W).

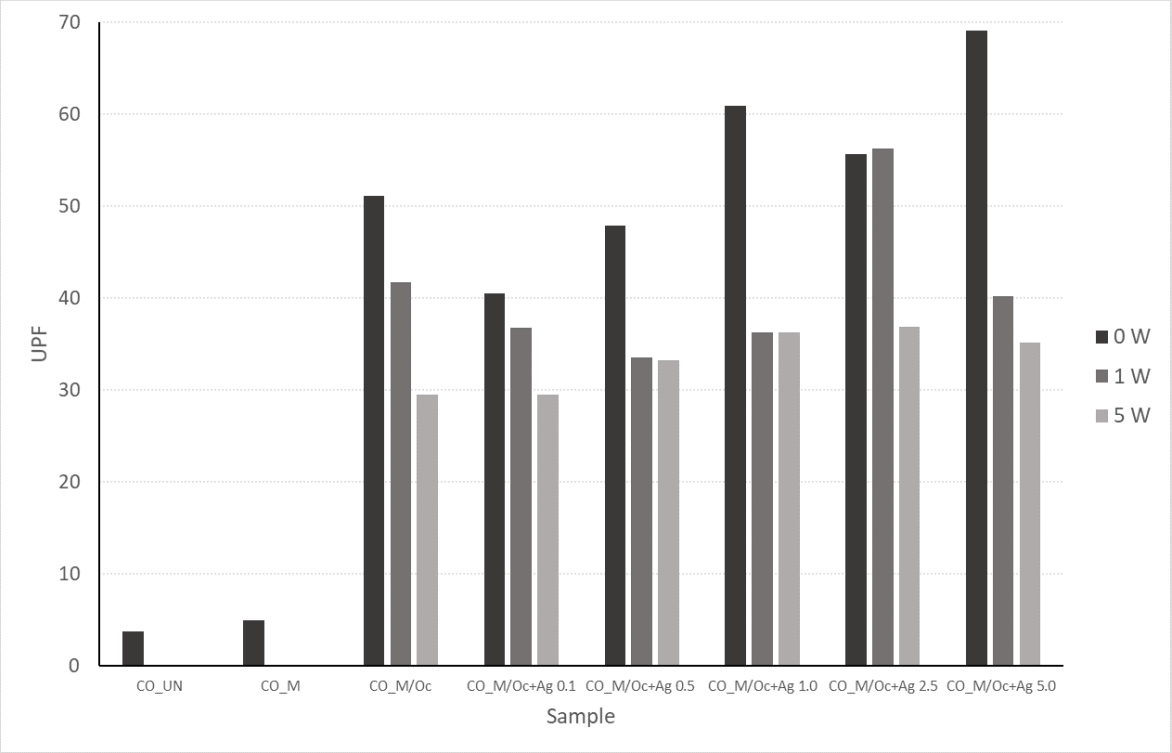

Figure 3.12: Ultraviolet protective factor, UPF, of the untreated and treated cotton samples before (0 W) and after one (1 W) and 5 repetitive washings (5 W).

Presence of Ag NPs influenced slight decrease of the UV protection properties, but only at lower studied concentrations of the $AgNO_3$. Accordingly, in comparison to the CO_M/OC sample, UPF of the samples CO_M/Oc+0.1Ag and CO_M/Oc+0.5Ag slightly decreased, but still demonstrating an excellent UV protection with an UPF higher than 40.0. Nevertheless, synergism between sumac extract and Ag NPs can be clearly observed in the case of the samples CO_M/Oc+1.0Ag, CO_M/Oc+2.5Ag and CO_M/Oc+5.0Ag, treated with higher studied concentrations of $AgNO_3$ in the synthesis bath. Compared with the CO_M/Oc sample, these samples exhibited greater UV protection performance, showing UPF values above 55.7. Accordingly much lower UV transmittance was detected, which in general decreased as the Ag content on the cotton fabrics increased.
To gain better insight into the mechanism of UV protection between CO_M/Oc sample and samples additionally treated with $AgNO_3$, measurements of reflection and transmission of the studied samples in the UV-vis region were obtained. Results in Figure 3.13 - 3.14 confirmed our assumption regarding the UV absorption ability of the CO_M/Oc sample ascribed to the presence of aromatic phenolic compounds in the sumac leaf extract. Namely, from both transmission and reflective curves of the CO_M/Oc sample, significant decrease of transmission and reflection can be observed in the UV spectral region, while both gradually increase by increase of the wavelength into the visible light spectrum (400–800 nm). These results undoubtedly confirm UV absorption action of the aromatic phenolic compounds within the sumac leaf extract. Besides, in comparison to the untreated cotton sample, decrease of the transmission and reflection properties of the CO_M/Oc sample in the lower wavelengths of visible light can also be detected, which has occurred due to absorption by the yellow pigments of the sumac leaf extract. In contrast, transmission and reflection of the CO_M/Oc+2.5Ag and CO_M/Oc+5.0Ag samples, treated with the highest studied concentrations of $AgNO_3$, significantly decreased and were very low in both, UV and visible spectra region. While transmission even at 780 nm did not exceed 10%, also the reflection remained low, i.e. less than 40%. Accordingly, at

higher concentration newly synthesised Ag NPs acted as an absorber in the whole measured spectral region. Moreover, closer examination of both transmission and reflection curves in the UV region revealed, that compared to the sumac leaf extract (sample CO_M/Oc), the presence of Ag NPs improved UV-protection in the UVA region. Namely, by increasing the Ag content on the cotton fibers, transmission and reflection in the 320–400 nm spectral region gradually decreased, until reaching the same values as CO_M/Oc sample in the UVB region.
UV protection properties of the studied samples decreased after one (1 W) and five (5 W) washing cycles (Table 3.2 and Figure 3.12), which is in accordance to the results of antibacterial activity as well as colour fastness. Accordingly, the reason for a decrease of the UPF values of the washed samples can be ascribed to desorption of the sumac leaf extract and Ag NPs from the cotton fibres after each washings. However, for most of the Ag treated samples it is possible to observe that the UPF decreased after first washing cycle, but remained practically the same after five washings. Therefore, Ag treated samples showed UPF values between 30 and 40, providing from good to excellent UV-protection even after five laboratory washings, which is equal up to twenty five domestic washings (i.e. according to the ISO 105-C06 standard method one laboratory washing equals five domestic washings). From this outcome, it is possible to assess the good laundering durability of the Ag treated textile samples due to durable attachment of the Ag NPs to the silica matrix deposited on cellulose fibres.

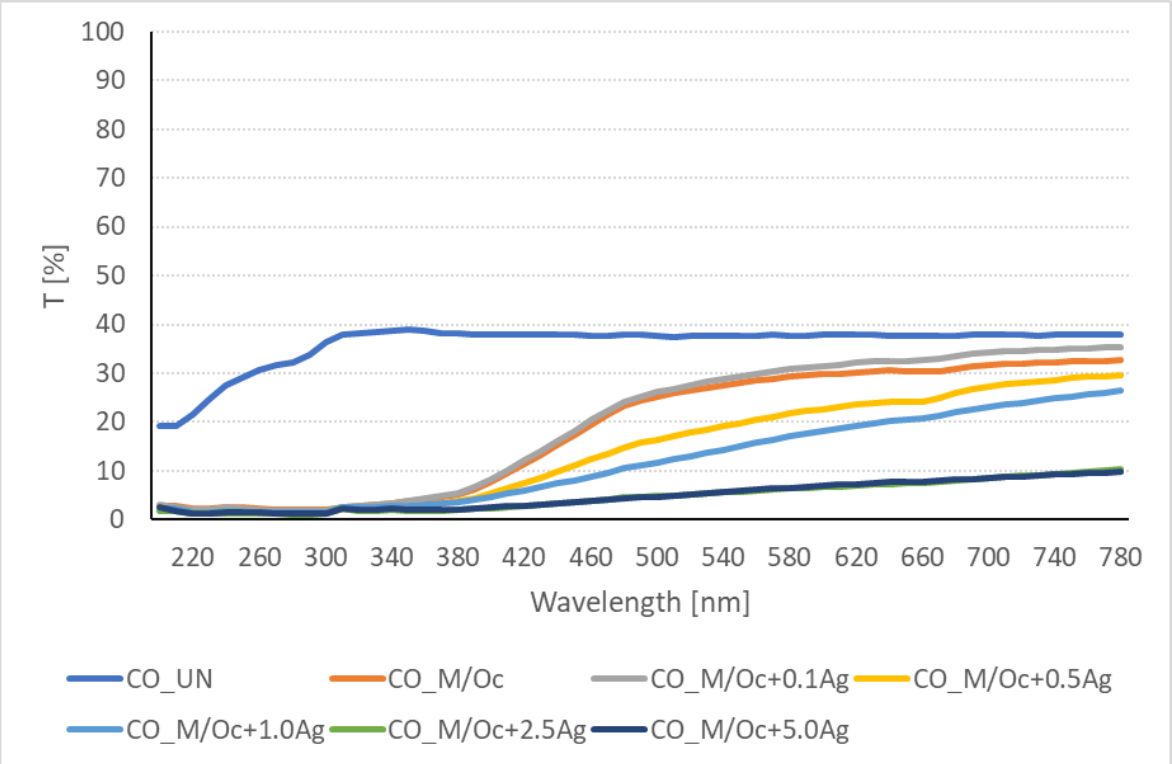

Figure 3.13: UV-vis transmission (T) spectra for untreated and Ag treated cotton samples.

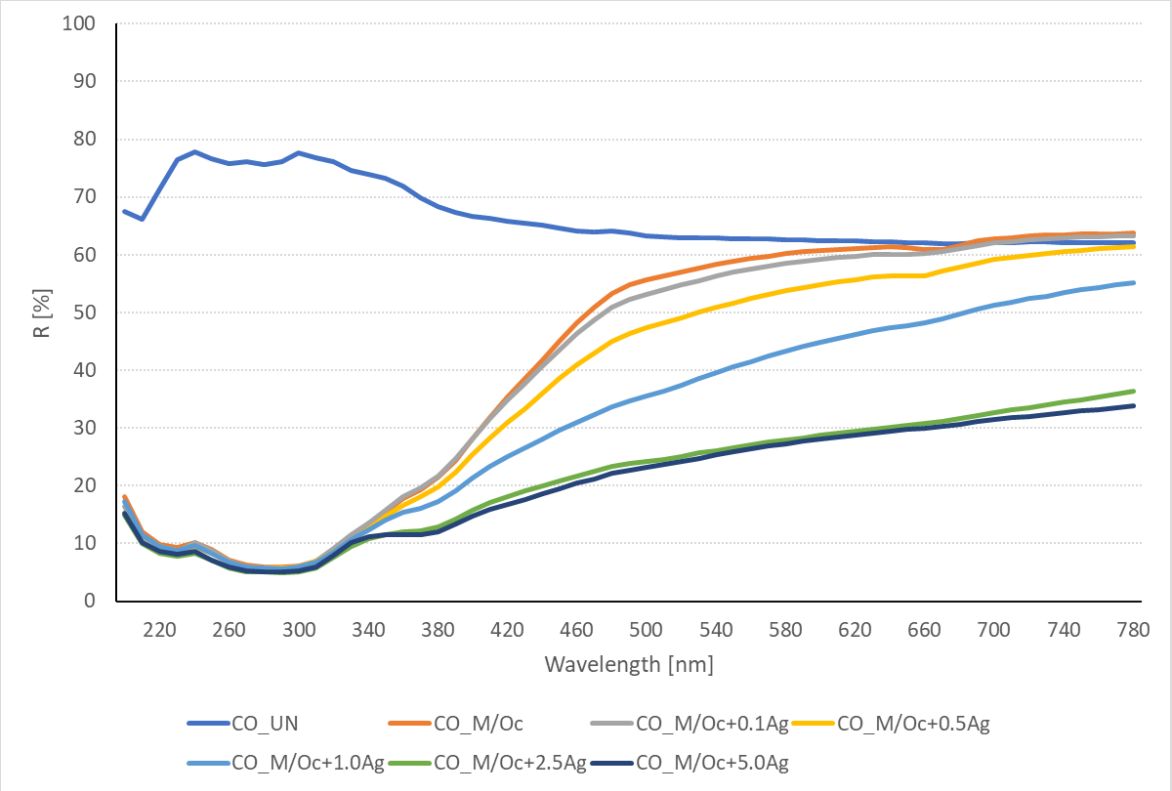

Figure 3.14: UV-vis reflection (R) spectra for untreated and Ag treated cotton samples.

Conclusion

In this research an antimicrobial and UV-protective coating has been successfully created on cellulose fibres using one step in situ synthesis of Ag NPs in the presence of an extract of sumac leaves, which was used as a reducing and capping agent. Ag NPs were successfully synthetized at different concentration of $AgNO_3$ and accordingly, difference in morphological and functional properties were investigated.

The different spectroscopic techniques like SEM, EDX, and ICP-MS confirmed the efficient and uniform deposition of spherical Ag NPs on the cotton surface. Silver concentration on cotton fibres increased with the increase of the silver salt concentration used, and the dimension of the formed cluster as well, going from fine NPs of 70 nm with 0.5 mM $AgNO_3$ to more than 100 nm with 5.0 mM $AgNO_3$, with growing particle size distribution. After washing the concentration of silver nanoparticles decrease in all the analysed samples.

Colorimetric analysis revealed that sumac leaf extract coloured the cellulose fibres with a pale yellow, and the conversion of Ag cations to Ag NPs caused the fibre to be coloured in deep brownish hue. Determination of ΔE^* between washed and unwashed samples confirmed rather poor colour fastness of the samples, especially due to the fast desorption of sumac extract.

The silver-treated cotton fabrics showed excellent antimicrobial effect against both *S. aureus* and *E. coli* with value of bacteria reduction superior to 97% even with lower concentrations of silver. The sumac leaf extract exhibited good antibacterial activity against *S. aureus* but appeared to be the perfect breeding ground for *E. coli* growth. Accordingly, higher MIC was determined for *E. coli* than *S. aureus*, while equal MBC of 340 mg/kg of Ag was determined regardless of the bacteria type. Washing fastness of the newly synthesized Ag NPs was concentration dependent, meaning the higher the initial concentration of the Ag NPs, the higher the retained antimicrobial activity after washing. In this respect, five consecutive washings resulted in loss of a sufficient protection against *E. coli*, while excellent antibacterial activity against *S. aureus* with a value of R>90% was still preserved for the sample treated with the highest studied concentration of $AgNO_3$ in the synthesis bath.

The sumac leaf extract provided high UV-protection, with a UPF value equal to 51.11. UPF reached higher value, if Ag NPs were present on the cellulose fibres, but only when treated with concentrations of $AgNO_3$ superior than 1.0 mM. In this cases Ag NPs acted as UV absorber, improving UV protection gained by sumac leaf extract by decreasing transmission and reflection in the UVA spectral region. In this respect synergistic activity between sumac leaf extract and Ag NPs was achieved. Washing of the samples resulted in a slight decrease of UV protection. Accordingly, even after five laboratory washings good to excellent UV protection with an UPF>30 was obtained.

The present study suggests that sumac leaf extract would be advantageous as a new type of reducing and stabilizing agent for chemical processing of Ag NPs loaded cotton. The process is distinguished by simplicity, efficiency, cost-effectiveness and environmental compatibility. The extract itself showed beautiful yellow hue, excellent antibacterial activity and high UPF value but its washing durability is not granted. Interesting investigations could be carried on exploring how variation of the aqueous extract concentration in chemical reduction could influence size and shape of the resulting NPs. Fur-

thermore, if excellent antibacterial and UV-protective properties were performed by unwashed silver treated cotton samples, further researches are warranted for improving the stability of Ag NPs on fibres during washing. The binding through physical interactions of the Ag NPs to the silica matrix improved the washing fastness of Ag NPs in terms of assuring UV-protection even after five laboratory washing which are according to the standard method used, equal to twenty-five domestic washings, but did not sufficiently prevent Ag NPs from leaching to impart washing durable antimicrobial activity against Gramm-negative bacteria, which was however obtained for the Gramm-positive bacteria. Therefore, new techniques of pre-treatment of textile fibres should be investigated to increase the adsorption of Ag NPs and stabilize their embedment in the fibres as well as control their release from fibres surface, completely preserving the washing fastness of the coating.

Bibliography

[Abbasi et al., 2016] Abbasi, E., Milani, M., Aval, S. F., Kouhi, M., Akbarzadeh, A., Nasrabadi, H. T., Nikasa, P., Joo, S. W., Hanifehpour, Y., Nejati-Koshki, K., and Samiei, M. (2016). Silver nanoparticles: Synthesis methods, bioapplications and properties. *Critical Reviews in Microbiology*, 42(2):173–180.

[Agnihotri et al., 2014] Agnihotri, S., Mukherji, S., and Mukherji, S. (2014). Size-controlled silver nanoparticles synthesized over the range 5–100 nm using the same protocol and their antibacterial efficacy. *RSC Adv.*, 4:3974–3983.

[Ahmed et al., 2016] Ahmed, S., Saifullah, Ahmad, M., Swami, B. L., and Ikram, S. (2016). Green synthesis of silver nanoparticles using Azadirachta indica aqueous leaf extract. *Journal of Radiation Research and Applied Sciences*, 9:1–7.

[Akter et al., 2018] Akter, M., Sikder, M. T., Rahman, M. M., Ullah, A. A., Hossain, K. F. B., Banik, S., Hosokawa, T., Saito, T., and Kurasaki, M. (2018). A systematic review on silver nanoparticles-induced cytotoxicity: Physicochemical properties and perspectives. *Journal of Advanced Research*, 9:1–16.

[Aladpoosh et al., 2014] Aladpoosh, R., Montazer, M., and Samadi, N. (2014). In situ green synthesis of silver nanoparticles on cotton fabric using Seidlitzia rosmarinus ashes. *Cellulose*, 21:3755–3766.

[AS/NZS, 2017] AS/NZS (2017). Sun protective clothing— Evaluation and classification. AS/NZS 4399:2017, Australian/New Zealand Standard, Sydney, Wellington: Standards Australia, Standards New Zeland.

[ASTM, 2001] ASTM (2001). Standard Test Method for Determining the Antimicrobial Activity of Immobilized Antimicrobial Agents Under Dynamic Contact Conditions (Withdrawn 2010). ASTM E2149-01, American Society for Testing and Materials International, West Conshohocken: ASTM International.

[Baghizadeh et al., 2015] Baghizadeh, A., Ranjbar, S., Gupta, V. K., Asif, M., Pourseyedi, S., Karimi, M. J., and Mohammadinejad, R. (2015). Green synthesis of silver nanoparticles using seed extract of Calendula officinalis in liquid phase. *Journal of Molecular Liquids*, 207:159–163.

[Baker et al., 2005] Baker, C., Pradhan, A., Pakstis, L., Pochan, D. J., and Shah, S. I. (2005). Synthesis and Antibacterial Properties of Silver Nanoparticles. *Journal of Nanoscience and Nanotechnology*, 5(2):244–249.

[Berger-Schunn, 1994] Berger-Schunn, A. (1994). *Practical color measurement*. New York: John Wiley & Sons.

[Borsa, 2012] Borsa, J. (2012). Antimicrobial natural fibres. In Kozlowski, R. M., editor, *Handbook of natural fibres*, pages 428–466. Woodhead Publishing.

[Cheng et al., 2011] Cheng, Y., Yin, L., Lin, S., Wiesner, M., Bernhardt, E., and Liu, J. (2011). Toxicity Reduction of Polymer-Stabilized Silver Nanoparticles by Sunlight. *J. Phys. Chem. C*, 115:4425–4432.

[Choi and Hu, 2008] Choi, O. and Hu, Z. (2008). Size Dependent and Reactive Oxygen Species Related Nanosilver Toxicity to Nitrifying Bacteria. *Environ. Sci. Technol.*, 42(12):4583–4588.

[Dhende et al., 2012] Dhende, V. P., Hardin, I. R., and Locklin, J. (2012). Durable antimicrobial textiles: types, finishes and applications. In *Understanding and improving the durability of textiles*, pages 145–173. Woodhead Publishing.

[Dring, 2003] Dring, I. (2003). Anti–microbial, rot-proofing and hygiene finishes. In Heywood, D., editor, *Textile Finishing*, page 351–371. Society of Dyers and Colourists.

[Du and Gebicki, 2004] Du, J. and Gebicki, J. M. (2004). Proteins are major initial cell targets of hydroxyl free radicals. *The International Journal of Biochemistry Cell Biology*, 36:2334–2343.

[Elsner, 2006] Elsner, P. (2006). Antimicrobials and the Skin Physiological and Pathological Flora. In Hipler, U. C. and Elsner, P., editors, *Biofunctional Textiles and the Skin*, pages 35–41. Karger, Basel.

[Epstein et al., 2014] Epstein, M., Emri, I., Hartemann, P., Hoet, P., Leitgeb, N., Martinez, L. M., Proykova, A., Rizzo, L., Rodriguez-Farré, E., Rushton, L., Rydzynski, K., Samaras, T., Testai, E., and Vermeire, T. (2014). Opinion on Nanosilver: safety, health and environmental effects and role in antimicrobial resistance . Technical Report DOE-SLC-6903-1, Scientific Committee on Emerging and Newly Identified Health Risks.

[Feng et al., 2000] Feng, Q. L., Wu, J., Chen, G. Q., Cui, F. Z., Kim, T. N., and Kim, J. O. (2000). A mechanistic study of the antibacterial effect of silver ions on Escherichia coli and Staphylococcus aureus. *Journal of Biomedical Materials Research*, 52(4):662–668.

[Fernando et al., 2018] Fernando, S. S. N., Gunasekara, T. D. C. P., and Holton, J. (2018). Antimicrobial Nanoparticles: applications and mechanisms of action. *Sri Lankan Journal of Infectious Diseases*, 8(1):2–11.

[Gao and Cranston, 2008] Gao, Y. and Cranston, R. (2008). Recent Advances in Antimicrobial Treatments of Textiles. *Textile Research Journal*, 78(1):60–72.

[Haider and Kang, 2015] Haider, A. and Kang, I.-K. (2015). Preparation of Silver Nanoparticles and Their Industrial and Biomedical Applications: A Comprehensive Review. *Advances in Materials Science and Engineering*, Article ID 165257.

[He et al., 2014] He, W., Liu, Y., Wamer, W. G., and Yin, J.-J. (2014). Electron spin resonance spectroscopy for the study of nanomaterial-mediated generation of reactive oxygen species. *Journal of Food and Drug Analysis*, 22:49–63.

[Iyigundogdu et al., 2017] Iyigundogdu, Z. U., Demir, O., Asutay, A. B., and Sahin, F. (2017). Developing Novel Antimicrobial and Antiviral Textile Products. *Appl Biochem Biotechnol*, 181:1155–1166.

[Jeevanandam et al., 2018] Jeevanandam, J., Barhoum, A., Chan, Y. S., Dufresne, A., and Danquah, M. K. (2018). Review on nanoparticles and nanostructured materials: history, sources, toxicity and regulations. *Beilstein J. Nanotechnol.*, 9:1050–1074.

[Jha and Prasad, 2016] Jha, A. K. and Prasad, K. (2016). Green synthesis and antimicrobial activity of silver nanoparticles onto cotton fabric: An amenable option for textile industries. *Adv. Mater. Lett.*, 7(1):42–46.

[Kapoor et al., 2017] Kapoor, G., Saigal, S., and Elongavan, A. (2017). Action and resistance mechanisms of antibiotics: A guide for clinicians. *Journal of Anaesthesiology Clinical Pharmacology*, 33:300–5.

[Karamian and Kamalnejad, 2019] Karamian, R. and Kamalnejad, J. (2019). Green synthesis of silver nanoparticles using Cuminum cyminum leaf extract and evaluation of their biological activities. *J. Nanostruct.*, 9(1):74–85.

[Khan et al., 2019] Khan, I., Saeed, K., and Khan, I. (2019). Nanoparticles: Properties, applications and toxicities. *Arabian Journal of Chemistry*, 12:908–931.

[Khodashenas and Ghorbani, 2015] Khodashenas, B. and Ghorbani, H. R. (2015). Synthesis of silver nanoparticles with different shapes. *Arabian Journal of Chemistry*.

[Kossah et al., 2011] Kossah, R., Zhang, H., and Chen, W. (2011). Antimicrobial and antioxidant activities of Chinese sumac (Rhus typhina L.) fruit extract. *Food Control*, 22(1):128–132.

[Kumar et al., 2017] Kumar, R., Umar, A., Kumar, G., and Nalwa, H. S. (2017). Antimicrobial properties of ZnO nanomaterials: A review. *Ceramics International*, 43(5):3940–3961.

[Lee, 2009] Lee, S. (2009). Developing UV-protective textiles based on electrospun zinc oxide nanocomposite fibers. *Fibers and Polymers*, 10(3):295–301.

[Liao et al., 2019] Liao, C., Li, Y., and Tjong, S. C. (2019). Bactericidal and Cytotoxic Properties of Silver Nanoparticles. *International Journal of Molecular Sciences*, 20(449).

[Liu et al., 2006] Liu, Z., Guo, B., Hong, L., and Lim, T. H. (2006). Microwave heated polyol synthesis of carbon-supported PtSn nanoparticles for methanol electrooxidation. *Electrochemistry Communications*, 8:83–90.

[Lok et al., 2007] Lok, C.-N., Ho, C.-M., Chen, R., He, Q.-Y., Yu, W.-Y., Sun, H., Tam, P. K.-H., Chiu, J.-F., and Che, C.-M. (2007). Silver nanoparticles: partial oxidation and antibacterial activities. *J Biol Inorg Chem*, 12:527–534.

[Mafune et al., 2000] Mafune, F., ya Kohno, J., Takeda, Y., Kondow, T., and Sawabe, H. (2000). Formation and Size Control of Silver Nanoparticles by Laser Ablation in Aqueous Solution. *J. Phys. Chem. B*, 104(39):9111–9117.

[Martinez-Castanon et al., 2008] Martinez-Castanon, G. A., Nino-Martinez, N., Martinez-Gutierrez, F., Martinez-Mendoza, J. R., and Ruiz, F. (2008). Synthesis and antibacterial activity of silver nanoparticles with different sizes. *J. Nanopart. Res*, 10:1343–1348.

[Mohammadi et al., 2016] Mohammadi, S., Zarei, M., Zarei, M. M., and Salehi, I. (2016). Effect of Hydroalcoholic Leaves Extract of Rhus Coriaria on Pain in Male Rats. *Anesthesiology and Pain Medicine*, 6(1).

[Moreno-Garrido et al., 2015] Moreno-Garrido, I., Perez, S., and Blasco, J. (2015). Toxicity of silver and gold nanoparticles on marine microalgae. *Marine Environmental Research*, 111:60–73.

[Muthuswamy Sathishkumar, 2010] Muthuswamy Sathishkumar, Krishnamurthy Sneha, Y.-S. Y. (2010). Immobilization of silver nanoparticles synthesized using Curcuma longa tuber powder and extract on cotton cloth for bactericidal activity. *Bioresource Technology*, 101:7958–7965.

[Nasar-Abbas and Halkman, 2004] Nasar-Abbas, S. and Halkman, A. K. (2004). Antimicrobial effect of water extract of sumac (Rhus coriaria L.) on the growth of some food borne bacteria including pathogens. *International Journal of Food Microbiology*, 97:63–69.

[Ovais et al., 2018] Ovais, M., Khalil, A. T., Islam, N. U., Ahmad, I., Ayaz, M., Saravanan, M., Shinwari, Z. K., and Mukherjee, S. (2018). Role of plant phytochemicals and microbial enzymes in biosynthesis of metallic nanoparticles. *Applied Microbiology and Biotechnology*, 102:6799–6814.

[Patil et al., 2019] Patil, A. H., Jadhav, S. A., Gurav, K. D., Waghmare, S. R., Patil, G. D., Jadhav, V. D., Vhanbatte, S. H., Kadole, P. V., Sonawane, K. D., and Patil, P. S. (2019). Single step green process for the preparation of antimicrobial nanotextiles by wet chemical and sonochemical methods. *The Journal of the Textile Institute*.

[Prabhu and Poulose, 2012] Prabhu, S. and Poulose, E. K. (2012). Silver nanoparticles: mechanism of antimicrobial action, synthesis, medical applications, and toxicity effects. *International Nano Letters*, 2(32).

[Pratsinis et al., 2013] Pratsinis, A., Hervella, P., Leroux, J.-C., Pratsinis, S. E., and Sotiriou, G. A. (2013). Toxicity of Silver Nanoparticles in Macrophages. *small*, 9(15):2576–2584.

[Raghunath and Perumal, 2017] Raghunath, A. and Perumal, E. (2017). Metal oxide nanoparticles as antimicrobial agents: a promise for the future. *Annalen dInternational Journal of Antimicrobial Agents*, 49:137–152.

[Rao et al., 2019] Rao, A. V., Ashok, B., Mahesh, M. U., Subbareddy, G. V., Sekhar, V. C., Ramanamurthy, G. V., and Rajulu, A. V. (2019). Antibacterial cotton fabrics with in situ generated silver and copper bimetallic nanoparticles using red sanders powder extract as reducing agent. *International Journal of Polymer Analysis and Characterization*, pages 1–9.

[Ravindra et al., 2010] Ravindra, S., Mohan, Y. M., Reddy, N. N., and Raju, K. M. (2010). abrication of antibacterial cotton fibres loaded with silver nanoparticles via Green Approach. *Colloids and Surfaces A: Physicochemical and Engineering Aspects*, 367(1-3):31–40.

[Rayne and Mazza, 2007] Rayne, S. and Mazza, G. (2007). Biological activities of extracts from sumac (Rhus spp.): A review. *Plant Foods for Human Nutrition*, 62:165–175.

[Rehan et al., 2019] Rehan, M., Barhoum, A., Khattab, T. A., Gatjen, L., and Wilken, R. (2019). Colored, photocatalytic, antimicrobial and UV-protected viscose fibers decorated with Ag/Ag_2CO_3 and Ag/Ag_3PO_4 nanoparticles. *Cellulose*, 26:5437–5453.

[Ren et al., 2016] Ren, Y., Gong, J., Wang, F., Li, Z., Zhang, J., Fu, R., and Lou, J. (2016). Effect of dye bath pH on dyeing and functional properties of wool fabric dyed with tea extract. *Dyes and Pigments*.

[Saravanakumar et al., 2016] Saravanakumar, A., Peng, M. M., Ganesh, M., Jayaprakash, J., Mohankumar, M., and Jang, H. T. (2016). Low-cost and eco-friendly green synthesis of silver nanoparticles using Prunus japonica (Rosaceae) leaf extract and their antibacterial, antioxidant properties. *Artificial Cells, Nanomedicine, and Biotechnology*.

[Schindler and Hauser, 2004] Schindler, W. D. and Hauser, P. J. (2004). *Chemical finishing of textiles*. Woodhead Publishing.

[Shaheen and Aty, 2018] Shaheen, T. I. and Aty, A. A. A. E. (2018). In-situ green myco-synthesis of silver nanoparticles onto cotton fabrics for broad spectrum antimicrobial activity. *International Journal of Biological Macromolecules*, 118(Part B):2121–2130.

[Shahriari et al., 2017] Shahriari, M., Veisi, H., Hekmati, M., and Nemmati, S. (2017). In situ green synthesis of Ag nanoparticles on herbal tea extract (Stachys Lavandulifolia)-modified magnetic iron oxide nanoparticles as antibacterial agent and their 4-nitrophenol catalytic reduction activity.

[Sharma et al., 2017] Sharma, P., Pant, S., Rai, S., Yadav, R. B., Sharma, S., and Dave, V. (2017). Green synthesis and characterization of silver nanoparticles by Allium cepa L. to produce silver nano-coated fabric and their antimicrobial evaluation. *Appl Organometal Chem.*, 32(3).

[Simoncic and Klemencic, 2015] Simoncic, B. and Klemencic, D. (2015). Preparation and performance of silver as an antimicrobial agent for textiles: A review. *Textile Research Journal*, 0(00):1–14.

[Simoncic and Tomsic, 2017] Simoncic, B. and Tomsic, B. (2017). Recent Concepts of Antimicrobial Textile Finishes. In Mittal, K. and Bahners, T., editors, *Textile Finishing*, pages 3–68. Scrivener Publishing LLC.

[Singh et al., 2018] Singh, A., Singh, N. B., Afzal, S., Singh, T., and Hussain, I. (2018). Zinc oxide nanoparticles: a review of their biological synthesis, antimicrobial activity, uptake, translocation and biotransformation in plants. *J Mater Sci*, 53:185–201.

[Slavin et al., 2017] Slavin, Y. N., Asnis, J., Hafeli, U. O., and Bach, H. (2017). Metal nanoparticles: understanding the mechanisms behind antibacterial activity. *Journal of Nanobiotechnology*, pages 15–965.

[Stular et al., 2017] Stular, D., Jerman, I., Naglic, I., Simoncic, B., and Tomsic, B. (2017). Embedment of silver into temperature- and pH-responsive microgel for the development of smart textiles with simultaneous moisture management and controlled antimicrobial activities. *Carbohydrate Polymers*, 159:161–170.

[Sun and Tang, 2011] Sun, S.-S. and Tang, R.-C. (2011). Adsorption and UV Protection Properties of the Extract from Honeysuckle onto Wool. *Ind. Eng. Chem. Res.*, 50:4217–4224.

[Tomsic et al., 2008] Tomsic, B., Simoncic, B., Cvijn, D., Orel, B., Zorko, M., and Simoncic, A. (2008). Elementary nano sized silver as antibacterial agent on cotton fabric. *Tekstilec*, 51(7-9):199–215.

[Tran et al., 2013] Tran, Q. H., Nguyen, V. Q., and Le, A.-T. (2013). Silver nanoparticles: synthesis, properties, toxicology, applications and perspectives. *Advances in Natural Sciences: Nanoscience and Nanotechnology*, 4(033001).

[Tsuneda et al., 2004] Tsuneda, S., Aikawa, H., Hayashi, H., and Hirata, A. (2004). Significance of cell electrokinetic properties determined by soft-particle analysis in bacterial adhesion onto a solid surface. *Journal of Colloid and Interface Science*, 279:410–417.

[ul Islam et al., 2019] ul Islam, S., Butola, B., Gupta, A., and Roy, A. (2019). Multifunctional finishing of cellulosic fabric via facile, rapid in-situ green synthesis of AgNPs using pomegranate peel extract biomolecules. *Sustainable Chemistry and Pharmacy*, 12(100135).

[ul Islam et al., 2016] ul Islam, S., Butola, B. S., and Mohammad, F. (2016). Silver nanomaterials as future colorants and potential antimicrobial agents for natural and synthetic textile materials. *RSC Advances*, 6:44232–44247.

[Vanti et al., 2018] Vanti, G. L., Nargund, V. B., N, B. K., Vanarchi, R., Kurjogi, M., Mulla, S. I., Tubaki, S., and Patil, R. R. (2018). Synthesis of Gossypium hirsutum-derived silver nanoparticles and their antibacterial efficacy against plant pathogens. *Appl Organometal Chem.*, e4630.

[Wang et al., 2017] Wang, L., Hu, C., and Shao, L. (2017). The antimicrobial activity of nanoparticles: present situation and prospects for the future. *International Journal of Nanomedicine*, 12:1227–1249.

[Wang and Zhu, 2017] Wang, S. and Zhu, F. (2017). Chemical composition and biological activity of staghorn sumac (Rhus typhina). *Food Chemistry*, 237:431–443.

[Wei et al., 2015] Wei, L., Lu, J., Xu, H., Patel, A., Chen, Z.-S., and Chen, G. (2015). Silver nanoparticles: synthesis, properties, and therapeutic applications. *Drug Discovery Today*, 20(105).

[Xiu et al., 2012] Xiu, Z.-M., bo Zhang, Q., Puppala, H. L., Colvin, V. L., , and Alvarez, P. J. J. (2012). Negligible Particle-Specific Antibacterial Activity of Silver Nanoparticles. *Nano Lett.*, 12:42714275.

[Yu et al., 2020] Yu, Z., He, H., Liu, J., Li, Y., Lin, X., Zhang, C., and Li, M. (2020). Simultaneous dyeing and deposition of silver nanoparticles on cotton fabric through in situ green synthesis with black rice extract. *Cellulose*, 27:1829–1843.

[Zhang et al., 2015] Zhang, W., Li, Y., Niu, J., and Chen, Y. (2015). Photogeneration of Reactive Oxygen Species on Uncoated Silver, Gold, Nickel, and Silicon Nanoparticles and Their Antibacterial Effects. *Langmuir*.

[Zhang et al., 2007] Zhang, W., Qiao, X., and Chen, J. (2007). Synthesis of silver nanoparticles—Effects of concerned parameters in water/oil microemulsion. *Materials Science and Engineering B*, 142(1):1–15.

[Zhang et al., 2016] Zhang, X.-F., Liu, Z.-G., Shen, W., and Gurunathan, S. (2016). Silver Nanoparticles: Synthesis, Characterization, Properties, Applications, and Therapeutic Approaches. *Int. J. Mol. Sci.*, 17(1534).

[Zhang et al., 2009] Zhang, Z., Jiang, C., Zhang, J., Zhang, H., and Shi, L. (2009). Ecophysiological evaluation of the potential invasiveness of Rhus typhina in its non-native habitats. *Tree Physiology*, 29:1307–1316.

[Zhou et al., 2017] Zhou, Q., Lv, J., Ren, Y., Chen, J., Gao, D., Lu, Z., and Wang, C. (2017). A green in situ synthesis of silver nanoparticles on cotton fabrics using Aloe vera leaf extraction for durable ultraviolet protection and antibacterial activity. *Textile Research Journal*, 87(19):2407–2419.

[Zhou et al., 2014] Zhou, Y., Zhang, J., Tang, R.-C., and Zhang, J. (2014). Simultaneous dyeing and functionalization of silk with three natural yellow dyes. *Industrial Crops and Products*.